AMERICAN SOCIETY FOR MICROBIOLOGY | Journal of Virology®

GENOME REPLICATION AND REGULATION OF VIRAL GENE EXPRESSION

Novel Human Polyomavirus Noncoding Control Regions Differ in Bidirectional Gene Expression according to Host Cell, Large T-Antigen Expression, and Clinically Occurring Rearrangements

Elvis T. Ajuh,[a] Zongsong Wu,[a] Emma Kraus,[b,c] Fabian H. Weissbach,[a] Tobias Bethge,[a]* Rainer Gosert,[a,d] Nicole Fischer,[b] Hans H. Hirsch[a,d,e]

[a]Transplantation & Clinical Virology, Department of Biomedicine (Haus Petersplatz), University of Basel, Basel, Switzerland

[b]Institute of Medical Microbiology, Virology and Hygiene, University Medical Centre Hamburg-Eppendorf, Hamburg, Germany

[c]Heinrich Pette Institute, Leibniz Institute for Experimental Virology, Hamburg, Germany

[d]Division Infection Diagnostics, Department of Biomedicine (Haus Petersplatz), University of Basel, Basel, Switzerland

[e]Infectious Diseases & Hospital Epidemiology, University Hospital Basel, Basel, Switzerland

ABSTRACT Human polyomavirus (HPyV) DNA genomes contain three regions denoted the early viral gene region (EVGR), encoding the regulatory T-antigens and one microRNA, the late viral gene region (LVGR), encoding the structural Vp capsid proteins, and the noncoding control region (NCCR). The NCCR harbors the origin of viral genome replication and bidirectional promoter/enhancer functions governing EVGR and LVGR expression on opposite DNA strands. Despite principal similarities, HPyV NCCRs differ in length, sequence, and architecture. To functionally compare HPyV NCCRs, sequences from human isolates were inserted into a bidirectional reporter vector using dsRed2 for EVGR expression and green fluorescent protein (GFP) for LVGR expression. Transfecting HPyV NCCR reporter vectors into human embryonic kidney 293 (HEK293) cells and flow cytometry normalized to archetype BKPyV NCCR revealed a hierarchy of EVGR expression levels with MCPyV, HPyV12, and STLPyV NCCRs conferring stronger levels and HPyV6, HPyV9, and HPyV10 NCCRs weaker levels, while LVGR expression was less variable and showed comparable activity levels. Transfection of HEK293T cells expressing simian virus 40 (SV40) large T antigen (LTag) increased EVGR expression for most HPyV NCCRs, which correlated with the number of LTag-binding sites (Spearman's r, 0.625; $P < 0.05$) and decreased following SV40 LTag small interfering RNA (siRNA) knockdown. LTag-dependent activation was specifically confirmed for two different MCPyV NCCRs in 293MCT cells expressing the cognate MCPyV LTag. HPyV NCCR expression in different cell lines derived from skin (A375), cervix (HeLaNT), lung (A549), brain (Hs683), and colon (SW480) demonstrated that host cell properties significantly modulate the baseline HPyV NCCR activity, which partly synergized with SV40 LTag expression. Clinically occurring NCCR sequence rearrangements of HPyV7 PITT-1 and -2 and HPyV9 UF1 were found to increase EVGR expression compared to the respective HPyV archetype, but this was partly host cell type specific.

IMPORTANCE HPyV NCCRs integrate essential viral functions with respect to host cell specificity, persistence, viral replication, and disease. Here, we show that HPyV NCCRs not only differ in sequence length, number, and position of LTag- and common transcription factor-binding sites but also confer differences in bidirectional viral gene expression. Importantly, EVGR reporter expression was significantly modu-

Received 21 December 2017 **Accepted** 5 January 2018

Accepted manuscript posted online 17 January 2018

Citation Ajuh ET, Wu Z, Kraus E, Weissbach FH, Bethge T, Gosert R, Fischer N, Hirsch HH. 2018. Novel human polyomavirus noncoding control regions differ in bidirectional gene expression according to host cell, large T-antigen expression, and clinically occurring rearrangements. J Virol 92:e02231-17. https://doi.org/10.1128/JVI.02231-17.

Editor Lawrence Banks, International Centre for Genetic Engineering and Biotechnology

Address correspondence to Hans H. Hirsch, hans.hirsch@unibas.ch.

* Present address: Tobias Bethge, Centre of Laboratory Medicine, Kantonsspital Aarau, Aarau, Switzerland.

lated by LTag expression and by host cell properties. Clinical sequence variants of HPyV7 and HPyV9 NCCRs containing deletions and insertions were associated with increased EVGR expression, similar to BKPyV and JCPyV rearrangements, emphasizing that HPyV NCCR sequences are major determinants not only of host cell tropism but also of pathogenicity. These results will help to define secondary HPyV cell tropism beyond HPyV surface receptors, to identify key viral and host factors shaping the viral life cycle, and to develop preclinical models of HPyV persistence and replication and suitable antiviral targets.

KEYWORDS polyomavirus, noncoding control region, early viral gene region, late viral gene region, T antigen, bidirectional, rearrangement

Polyomaviruses (PyVs) belong to the *Polyomaviridae*, which are characterized by the restricted range of hosts that they can productively infect (1). PyV virions are nonenveloped icosahedral particles of approximately 45 nm in diameter containing a circular, double-stranded DNA genome of about 5 kb (1, 2). More than 70 PyVs have been identified to date, and at least 13 are described as human polyomaviruses (HPyVs) (3). In 1971, isolation of PyV BK (BKPyV) and PyV JC (JCPyV) by cell culture was reported from urine of a kidney transplant patient and from brain tissue of a patient with progressive multifocal leukoencephalopathy (PML), respectively (4, 5). In the past decade, molecular techniques have led to the discovery of 11 novel HPyVs, called Karolinska Institute polyomavirus (KIPyV) (6), Washington University polyomavirus (WUPyV) (7), Merkel cell polyomavirus (MCPyV) (8), human polyomavirus 6 (HPyV6) (9), human polyomavirus 7 (HPyV7) (9), trichodysplasia spinulosa polyomavirus (TSPyV) (10), human polyomavirus 9 (HPyV9) (11), human polyomavirus 10 (HPyV10) (12), St. Louis polyomavirus (STLPyV) (13), human polyomavirus 12 (HPyV12) (14), and New Jersey polyomavirus (NJPyV) (15). While this work was in progress, Lyon IARC PyV (LIPyV) has been described, awaiting further confirmation as an HPyV (16).

The molecular detection of HPyV genomes has been complemented by important serological evidence of infection using HPyV Vp1 capsid-specific IgG antibodies. The results indicated that HPyV infections frequently occur during childhood, reaching high seroprevalence rates of 40% to 90% in the general adult population, with average coexposure rates of 6 to 7 HPyVs (17–19). Despite this high rate, clinical symptoms or signs of primary HPyV infection have not been identified. In fact, only 5 HPyVs have been consistently linked to disease: BKPyV to nephropathy and hemorrhagic cystitis (20–22), JCPyV to PML and nephropathy (23), MCPyV to Merkel cell carcinoma (8), TSPyV to trichodysplasia spinulosa (10), and HPyV7 to pruritic hyperproliferative keratinopathy (24). HPyV diseases occur almost exclusively in patients with inherited, acquired, or therapeutic immunodeficiency states such as transplantation, HIV-AIDS, autoimmune disease, and cancer/chemotherapy (3, 25, 26). Evidence of HPyV disease is emerging for KIPyV (27), WUPyV (28, 29), HPyV6 (30, 31), HPyV10 (12), and NJPyV-2013 (15) due to dedicated studies correlating histopathology and virus infection by specific immunohistochemistry.

Despite this plethora of different HPyVs, their genome organizations are similar and can be divided into three functional regions: the early viral gene region (EVGR), encoding the regulatory large T antigen (LTag) and small T antigen (sTag) and various spliced derivatives as well as microRNAs (miRNAs); the late viral gene region (LVGR), encoding the structural Vp capsid proteins; and the noncoding control region (NCCR), harboring the origin of viral replication and bidirectional promoter/enhancer functions governing EVGR and LVGR expression in opposite directions on opposite DNA strands, and which contains numerous transcription factor-binding sites (TFBS) (1, 3, 32, 33). Of note, rearrangements of the archetype BKPyV NCCR and JCPyV NCCR have been identified in patients with nephropathy (34) and PML (23, 35), respectively, and were shown to confer high EVGR expression, augmented viral replication capacity, and increased cytopathology compared to their nonrearranged archetype counterparts (34, 36, 37). However, systematic functional comparisons of novel HPyV replication and their

rearranged variants have not been reported so far. In fact, cell culture propagation of the novel HPyVs has been difficult, which severely limits studies of viral replication and antiviral targets. However, HPyV-host cell interactions have been studied at the level of viral capsid-receptor interactions defining primary HPyV cell tropism and entry (32, 38–40). Yet, the NCCR defines a second level of host cell tropism after delivery of the viral genome into the nucleus, which is critical for coordinating and directing decisions regarding latency/persistence as well as progression through the viral life cycle (33). To experimentally overcome the NCCR bottleneck, researchers have resorted to viral recombinants carrying genomes with hybrid NCCRs, e.g., between SV40 and JCPyV (41, 42), or have provided SV40 EVGR proteins like the LTag in *trans* (43–46). To study the role of specific TFBS in archetype and rearranged HPyV NCCRs, we have chosen the archetype BKPyV NCCR as a model and introduced inactivating point mutations in 28 common TFBS (47). We identified three phenotypic groups of (i) strong, (ii) intermediate, or (iii) low EVGR expression and the corresponding viral replication capacities (47). Interestingly, a prominent role emerged for the TFBS of rather common host cell factors such as Sp1, Ets1, and NF1 (47). Indeed, Sp1 was recently identified as essential for progressing into EVGR expression by whole-genome RNA interference screen (see Table S2 in reference 48). However, point mutation analysis identified two key Sp1 sites, one each in the EVGR and the LVGR promoters, where they exerted different functions based on their location, directionality, and affinity and conferred graded activation of EVGR expression at the expense of LVGR expression (49). When examining archetype NCCRs of the HPyVs, we found differences not only in NCCR length but also in the number and the composition of common TFBS and LTag binding sites. We therefore hypothesized that these NCCR differences give rise to different bidirectional EVGR and LVGR expression patterns. To this end, our results indicate the presence of a hierarchy of HPyV EVGR expression, which is modulated by host cell, LTag expression, and clinically occurring NCCR rearrangements.

(Parts of the results from this study have been presented as poster P19-1 on the occasion of the 6th Congress of the European Society of Virology, in Hamburg, Germany, 21 October 2016.)

RESULTS

HPyV NCCRs confer different strengths of EVGR expression. Given the prominent role of Sp1, Ets1, NF1, and LTag in the archetype BKPyV NCCR (33, 47, 49), we compared the archetype NCCRs of BKPyV, JCPyV, and 11 novel HPyVs and found differences not only in the overall length but also in the number and composition of these binding sites (50) (Fig. 1; Table 1).

LTag-binding sites were predicted in all HPyV NCCRs and preferentially located in the EVGR promoter region, numbering an average of 5, ranging from 1 and 2 for HPyV6 and HPyV7 to 10 and 12 for TSPyV and MCPyV NCCRs. NF1 sites were preferentially predicted in the LVGR, but some HPyV NCCRs had an average of one or less than one (MCPyV, HPyV6, HPyV7, HPyV9). Sp1, Ets1, and Spi-B sites were found in all HPyV NCCRs and often in clusters (Fig. 1).

We therefore hypothesized that these differences in NCCR confer different bidirectional EVGR and LVGR expressions. To test this hypothesis, we compared 13 archetype HPyV NCCRs using a novel bifluorescent reporter vector, pRG13D12, recapitulating the PyV genome organization regarding bidirectional EVGR and LVGR (Fig. 2A). To validate its suitability (Fig. 2B), NCCRs of the well-characterized archetype BKPyV(ww) and the rearranged BKPyV strain Dunlop (DUN) were inserted, and the resulting reporter constructs were transfected into HEK293 cells and analyzed by flow cytometry at 48 h posttransfection (hpt). Indeed, the rearranged BKPyV NCCR(DUN) conferred significantly stronger EVGR expression (shown in red) than did the archetype BKPyV(ww) NCCR, which was inversed in the reverse orientation (Fig. 2C), in line with previous results (34, 47). Quantification of the fluorescent cells (Fig. 2D) and the mean fluorescence intensity (MFI) indicated that the simplified reporter vector pRG13D12 captured

FIG 1 *In silico* prediction of common transcription factor- and LTag-binding sites in the NCCRs of 13 HPyVs. The BKPyVww NCCR was used as the reference as described in Materials and Methods (49). HPyV NCCR length is shown in the brackets in base pairs. The direction of EVGR and LVGR transcription and the start codon (ATG) are depicted in red and green arrows, respectively. TSS, transcription start sites (marked by dashed arrows); inr, initiation element (in gray rectangle); DPE, downstream promoter element (in blue rectangle). Binding sites are indicated as follows: red triangles, LTag; yellow triangles, Sp1; green triangles, NF-κB; black square, TATA box; gray square, TATA-like element; blue triangles, NF1; orange triangles, Ets1; light orange triangles, Spi-B; pink rectangles, origins of replication (ori).

these differences (Fig. 2E), hence being suitable for a principal comparative analysis of HPyV NCCRs.

To that end, 13 archetype HPyV NCCR sequences were inserted into pRG13D12, verified by sequencing, and transfected into human embryonic kidney (HEK293) cells. EVGR and LVGR expressions were quantified by flow cytometry, and the results were normalized to the archetype BKPyV NCCR(ww). The results demonstrated that EVGR expression in HEK293 cells varied over more than 3 orders of magnitude (Fig. 3A). MCPyV and HPyV12 NCCRs were located at the upper end of the EVGR responses, whereas HPyV6 and HPyV9 NCCRs were found at the lower end. The corresponding LVGR expression also showed some variability but tended to be within the same order of magnitude (Fig. 3A). The results indicated that HPyV NCCRs gave rise to a hierarchy of EVGR expression levels in HEK293, which were higher than, similar to, and lower than the corresponding archetype BKPyV NCCR activity in HEK293.

LTag activates HPyV NCCR-controlled EVGR expression. Since LTag is a major regulatory protein encoded by the EVGR and exerts key functions in viral replication and gene expression, parts of which are mediated directly through LTag-binding sites (Fig. 1, red triangles), it was of interest to investigate the effect of LTag on HPyV NCCR reporter expression. To ensure comparable conditions for all 13 HPyV NCCRs, the well-characterized HEK293 derivative 293T cells were chosen, which constitutively express SV40 LTag (49). Transfection and flow cytometry analysis 48 hpt showed that the overall hierarchy of EVGR expression was only little changed, whereby MCPyV and HPyV12 were in the higher group and HPyV6 and HPyV7 remained in the lower group (Fig. 3B). However, JCPyV EVGR expression appeared to be most responsive to SV40

TABLE 1 Nucleotide sequences of HPyV noncoding control region (NCCR)[a]

HPyV (GenBank accession number)	Sequence
BKPyV-DUN KP412983	CATTTTTGCAAAAATTGCAAAAGAATAGGGATTTCCCCAAATAGTTTTGCTAGGCCTCAGAAAAAGCCTCCACACCCTTACTACTT GAGAGAAAGGGTGGAGGCAGAGGCGGCCTCGGCCTCTTATATATTATAAAAAAAAAGGCCACAGGGAGGAGCTGCTT ACCCATGGAATGCAGCCAAACCATGACCTCAGGAAGGAAAGTGCATGACTCACAGGGGAATGCAGCCAAACCATGA CCTCAGGAAGGAAAGTGCATGACTCACAGGGAGGAGCTGCTTACCCATGGAATGCAGCCAAACCATGACCTCAGGAA GGAAAGTGCATGACAGACATGTTTTGCGAGCCTAGGAATCTTGGCCTTGTCCCCAGTTAAACTGGACAAAGGCCATG
BKPyVww JQ513592	CATTTTTGCAAAAATTGCAAAAGAATAGGGATTTCCCCAAATATTTTTGCTAGGCCTCAGAAAAAGCCTCCACACCCTTACTACTT GAGAGAAAGGGTGGAGGCAGAGGCGGCCTCGGCCTCTTATATATTATAAAAAAAAAGGCCACAGGGAGGAGCTGCTA ACCCATGGAATGTAGCCAAACCATGACCTCAGGAAGGAAAGTGCATGACTGGGCAGCCAGCCAGTGGCAGTTAATAG TGAAACCCCGCCCCTGAAATTCTCAAATAAACACAAGAGGAAGTGGAAACTGGCCAAAGGAGTGGAAAGCAGCCAGA CAGACATGTTTTGCGAGCCTAGGAATCTTGGCCTTGTCCCCAGTTAAACTGGACAAAGGCCATG
JCPyV AB038249	CATTTTAGCTTTTTGCAGCAAAAAATTAGTGCAAAAAAGGGAAAAACAAGGGAATTTCCCTGGCCTCCTAAAAAGCCTCCACGCC CTTACTACTTCTGAGTAAGCTTGGAGGCGGAGGCGGCCTCGGCCTCCTGTATATATAAAAAAAAGGGAAGGTAGGGAG GAGCTGGCTAAAACTGGATGGCTGCCAGCCAAGCATGAGCTCATACCTAGGGAGCCAACCAGCTGACAGCCAGAGGG AGCCCTGGCTGCATGCCACTGGCAGTTATAGTGAAACCCCTCCCATAGTCCTTAATCACAAGTAAACAAAGCACAAGG GGAAGTGGAAAGCAGCCAGGGGAACATGTTTTGCGAGCCAGAGCTGTTTTGGCTTGTCACCAGCTGGCCATG
KIPyV EF127906	CATTTTGCCTCTCTAGGCCTCTCAAATGCCTCTGCAGGCCCTCTCCTTCTTCTAGAAAAAGCTGGGGCTTTTTTGGCCTCTGG CCTCCTGTAATATAGAAAAAAAGGGCACAGTGATTGACAGTTGTGTATACAAGCATGTGTGGTATGTTTAGTGTGTAAG CCAATAAAGTTAAAGGTCACTACTGTGGGTGGTGACACCTGATACCGGCGGAACTAGTTGCTACGTGCCACACAATAGC TTTCACTCTTGGCGTGAAGCCAACTTCCTGGGCCGTGAGCCAGCTTCCTGCGGCCTTGTGTTTTTTACCAACACACCTGGT GAACTTCTACTGTCCTTGACACAGGTAAGACTGGGGACCCTTTGTAGGCCAAAGGAGAGTGAAGGGTAACTGAAATGC TAAGACTGTAAGTTCTAATCCTAGTATTTCAGTTCGGGGATGTT GGCGCCATCGTCTCGAACCTGGCCTGCATACCTTT GGATATAGAGGGTCACCAATTTTTATTTTGTTTTTAGATG
WUPyV NC_009539	CATTTTGCCTTCTTTAGCCTCAAGGCGCCTCAGCAAGGCCCTCTGCTTTTAGTTCAGAAAGTTGAGGCTTTTTAGGCCTCAGGCCT CCTTATTATAATAAAAAAAAGCTAAGCATGATTGACAGTGTGGGCTAAACCAAAAGCACAAGAACAAAGCTTTTAGCC AATTAGCAGCCACAAGGTGGAGCAAAAGTATTAAGTTTCACTGTTATGTGCAGGAATGTGCAGCTGTGACCTTTTAAAG TTTCCGGGCACGGCGCCAACTTCCTGGGCCTGGTGCCATACCAACACAGCTGCTGAGCTTCCGGAATACAATACTGGTG CCCTTTGTAAGTGTTTTACAGGTAAGTAAGGCCTACAACAGGGCTTATTTGTACTATAAGTTAATGGGGGCCCTTTGTAG TCCAGCGGAAAGTGAAGGGTGGCTTAACAGAGACGTCCTTGGGTTCAAACCTAAGGGTGCCATAAGCAACATTACATT AATGTTGTGACATCTCCAGTCGGGGGTATTGGCCTATAGGAAACCCTAGGGCTCTATAAGCAGCATACATAT GTTGT GACATCTCCGTTGAGTCTGGGGGTATTGGTGCTACCGTCTCGAACCTAGCCGACAGCCGTTGGATATAAAGGGTCACCATT TTTATTTCAGATG
MCPyV-R17b HM011556	CATCTTGTCTATATGCAGAAGGAGTTTGCAGAAAGAGCAGAGGAGCAAATGAGCTACCTCACTAAGGAGTGGTTTTTATAC TGCAGTTTCCCGCCCTTGGGATCTGCCCTTAGATACTGCCTTTTTTGCTAATTAAGCCTCTTAAGCCTCAGAGGCCTCTCTC TTTTTTTTCCAGAGGCCTCGGAGGCTAGGAGCCCCAAGCCTCTGCCAACTTGAAAAAAAAAAGTCACCTAGGCAGCCA AGTTGTGGTTACATGATTGAACTTTTATTGCTGCAGGGTTTCTGGCATTGACTCATTTCCTGGAGAGGCGGAGTTTGACT GATAAACAAAACTTTTTTTCTTTCTGTTTGGGAGGGAGACGGAAGACTCTTAACTTTTTTTCAACAAGGGAGGCCCGGAG GCTTTTTTTTCTCTTACAAAGGGAGGAGGACATTAAAAGAGTAA GTATCCTTATTTATTTTTCAGGATG
MCPyV-MCV156 HM355825	CATCTTGTCTATATGCAGAAGGAGTTTGCAGAAACAGCAGAGGAGCAAATGAGCTACCTCACTAAGGAGTGGTTTTTATAC TGCAGTTTCCCGCCCTTGGGATCTGCCCTTAGATACTGCCTTTTTTGCTAATTAAGCCTCTTAAGCCTCAGAGGCCTCTCTCT TTTTTTTCCAGAGGCCTCGGAGGCTAGGAGCCCCAAGCCTCTGCCAACTTGAAAAAAAAAAGTCACCTAGGCAGCCAAG TTGTGGTTACATGATTGAACTTTTATTGCTGCAGGGTTTCTGGCATTGACTCATTTCCTGGAGAGGCGGAGTTTGACTGA TAAACAAAACTTTTTTTCTTTCTGTTTGGGAGGGAGACGGAAGACTCTTAACTTTTTTTCAACAAGGGAGGCCCGGAGG CTTTTTTTTCTCTTACAAAGGGAGGAGGACATTAAAAGAGTAAG TATCCTTATTTATTTTTCAGGATG
HPyV6 HM011563	CATTTTGCTGCTTGAGTAGTCTCTGAATGAAATGTTAAAATCCCAGACAGCAGGTGAAATCCCTGTGCAGGCTTACGCAACTG GGCAGGGCCATTTAAGCTCCCTTATCTCTCTAATTATAGGAGGCAATAAAGGCCACCAGGCCACCTCAATGTATGAGAA AAAAGGAGAGGAAATAGGGCAACCAAAGGTCAAAAGGAAGTTATTAGGCGAGAAAAGCCCGCCAAATTTTTTCCCA GTCATAACTGAGGTTGACCACCGTTGACACAACACCCTAATTAGTAAGTTCTTCAATTTCTGTTTTATTTTGTTTTAACTC TTCAGTGACCTCACCGCCTGTTGACCCTGGTCTTAATTTCTACTTAACAGGTAAGCCATG
HPyV7 HM011567	CATTTTCCCTTTCTCTCTGTAATTTCTGAAGAGAAAGTGGTGGCAGGTGCAGCTGACACCCTTTAAATAGTCTTCTCTCTGCAAT AGAAGGGTGGAGGCAAGAGGCCACCAAGCCACCTACATTAGGAAAAAAAAGGTGGAGGAGGAAATGTCTGGGTTAC TGGGTCAGACAGGATATGATTAGCATAATATTAGCCCGCCAAAAGCTGTGGTTTTTATGCAGATGAGGTGTGACCTTT GGTGGAGGACCTATCTCTCTATCTGTAAGTAAGAATTTTTCACTTTTTAACAAATTTTAACCTCTTAGTAACTGTAGTGTT CTCTCTCCTCAGAAAGTCCTTGATATTGTTGGCCATTTGGGTGCTGTGTCAAGGACTTAGGTAAGAGAATG
HPyV7-PITT1 KJ733012	CATTTTCCCTTTCTCTCTGTAATTTCTGAAGAGAAAGTGGTGGCAGGTGCAGCTGACACCCTTTAAATAGTCTTCTCTCTGCAATA GAAGGGTGGAGGCAACAGGCCACCAAGCCACCTACATTAGGAAAAAAAAGGTGGAGGAGGAAATGTCTGGGTTAC TAGGTCAGACAGGATATGATTCAGACAGGATATGATTAGCATAATATTAGCCCGCCAAAAAGTGGTTTTTATGCAGATG AGGTTTCACCTTTGGTGGAGGACCTATCTCTCTATCTGTAAGTAAGAATTTTTCACTTTTTAACAAATTTTAACCTCTTAG TAACTGTAGTTTTCTCTCTCCTCAGAAAGTCCTTGATATTGTTGGCCATTTGGGTGCTGTGTCAAGGACTTAGGTAAGAGAATG

(Continued on next page)

TABLE 1 (Continued)

HPyV (GenBank accession number)	Sequence
HPyV7-PITT2 KJ733013	CATTTTCCCTTTCTCTCTGTAATTTCTGAAGAGAAAGTGGTGGCAGGTGCAGCTGACACCCTTTAAATAGTCTTCTCTCTGCAATA GAAGGGTGGAGGCAAAAGGCCACCAAGCCACCTACATTAGGAAAAAAAAGGTGGAGGAGGAAATGTGTCAGACAG GATATGATTAGCATAATATTAGCCCGCCAAAAAGTGGTTTTTATGCAGATGAGGTTTCACCTTTGGTGGAGGACCTAT CTCTCTATCTGTAAGTAAGAATTTTTCACTTTTTAACAAATTTTAACCTCTTAGTAACTGTAGTTTTCTCTCTCCTCAGAAA GTCCTTGATATTGTTGGCCATTTGGGTGCTGTGTCAAGGACTTAGGTAAGAGAATG
TSPyV GU989205	CATTTTGCTGAATGCACCAGAAGACAGGTAAGGGGAGAAATGAAGAAATGAAGATGGGAGCTTTTTGGAGCCCTTTTAAAGCC TCTGTGTGCCTCAATTAATTTTCATCAGATTTGGCTTACATAAAAGGGAGGAAGTGCCAAGCCTCAAGAGGCCTCCGGA GGCCTCTCCCTCTATGTCTGTGTCAAGAGGGGGCAGGAAGCCTCAGCCTCCTGGTAATACTGAGAAAAAACAAGATTT CCATAGTAACCCCCTATTAGGAATTTGAGGAACTATACTTAGAGTGTTGACATAAATAGGTCATTGTTTGCTTAAGACCGTT ATCCTGAGGAAGCTCGTGCGCCACCTATCATTTGTTATGGAAAATGCTGTGTCAGTTAGTCTCAAGGGGATGTTTGTCA TACTGCCACAAACACAGGAAGGCAGCCAAGAGACAAGAGGAAGCCAGCCAAATCCCGTGATTGTTTTTGTATATTCTTAA GATAGCACTTGTCTAACTGCTCTCATCCTGTCCGTCCGGTCTCCATAACAACACATCCTCCCGCTCTGTGTT CTCACGC GGCAAATTCAAATTCTAATGGTAAGTTTTTCTTATTTTTCAGGTAAAATG
HPyV9 HQ696595	CATGGCTCTGCAAAAAGTAAAATAAGTCTTACTACCTGAGAATCAAGTTAATTAAGTTTCAAATAGGTGGAGAACTTCTTACCT TAATGAGTTTTGGAAAAGCCTCCAAAGCCTCTCTCTTTGTTGCAACAAGAGAAGGAGGCAAGGGGCCCCTGGCCTCTTAT ACTATCAAAAAAAAACCTGTGTTGCCATAGTGATTTTGAGTGACAGGGAGATAACTTTGCAAATTGAGGAACTAAATGAC AGGTTATTTTTGCAGAATCAACTCTAGAGGAAACTGTGGTATCTGTGGTATCTACCTGCTCCACTTGACTGCCTGGGGAC TTTTTGGTGACATTCCGGTGTGTGACAAACAAGTGCATTGCGGTTTCCGTTGCTAGGTGGCGCTTAGCAACCCCTCTAGA TACCAGTAGCTAAGGGGGAAGTGAAATCATTTTGCCATC TAAGGTCAACAGAGAAGAAGCCCGCCTAAACTA AACGCGCCAATTTTGAACTTGGGTAAGATATG
HPyV9-UF1 KC831440	CATGGCTCTGCAAAAAGTAAAATAAGTCTTACTACCTGAGAATCAAGTTAATTAAGTTTCAAATAGGTGGAGAACTTCTTACCTT AATGAGTTTTGGAAAAGCCTCCAAAGCCTCTCTCTTTGTTGCAACAAGAGAAGGAGGCAAGGGGCCCCTGGCCTCTTAT ACTATCAAAAAAAAACCTGTGTTGCCATAGTGATTTTGAGTGACAGGGAGATAACTTTGCAAATTGAGGAACTAAATGA CAGGTTATTTTTGCAGAATCAACTCTAGAGGAAGACTGTGGTATCTACCTGCTCCACTTGACCGCCCGGGGACTTTTTGGT GACATTCCGGTGTGTGACAAACAAGTGCATTGCGGTTTCCGTTGCTAGGTGGCGCTTAGCAACCCCTCTAGATACCAGT AGCTAAGGGGGAAGTGAAATCATAGCAACCTAGAGGAAG CTCATTTCATCAGCGCCGCCCAGAAGCCCGCCTT TTTTAAACCCGCCCATTTTGAACTTGGGTAAGATATG
HPyV10 JX262162	CATCCTTGCTGAATTTGCAAGTAGTAAAAAGTTTGCAGACGCGGTAAAGATGGCTCCCAGAGTCCTTCCTCTTTTCACCGGAAA GACAGAGGCTTAGGCCTCCGGCCCCCGGCTTATATAGAAAAAATTTTAGCTTATTGTTTTGCTACTTAACCTCAGGTAGG TCAACAGCTATTGTTGGCAAGCTATTGTTGGCAAGTATTGGTATTAATCACCCAGACAACTCAGAAGTTTCCACCTCTT GGAGGCGGTCCAGAGTTAACCTGTGACTGTTGGCGGGAAGCCAATAACAGCAACTTTGACATTTCATCACGAGCCCTT TAAACGCCCTCTAGGCGGAGACGGAAGACAATTGACTCTTGGCACGGACGGAAGAGGAATGCCGTCTGCTCAC CTTAGTTAACACGAGATTTTCTTTGGAAATACTCCAAAGTACAGTAAGTATATG
STLPyV JX463183	CATTGCTGCAGAGTCAACTTCTGTCTCTAAAGAGGCTGAGGCTTAGGCCCCAGGCCCCCGCATATATATGAGAAAAAAGGTAGC TGTGTGACTCACATTATTTATTGTCTATTGCATAGTTTCATCACCTCAGTGATTCTTGGCAGTTTGCCACCTGGCTGAAT CAGAGTGTGGAGCAGCTGCTGCGTGACCTGGAAAGCTGTCAAACCACGGAAAAGAGCGCCAAGGCAACCAATAGAC TTTGGCTCTGTGCCCCTAGGCACACCTTACTTCCGGATATTATATAGACCATAATATTTAGTCAGCTGAGAGTAGTAAC TTCGGCAGCGAGCCAACAACAGCATTATGTAAGTAAATG
HPyV12 JX308829	CATTCTGCTAAATTAGTGCAGTACAGTGTACGTGCCTGGTACCAAAAATGGCCTCCAAAAGCCTCTCCCTTTTTTTATAGGAAGGA CGGGGGCTGGGTGCCTCTTGCCTCCCAGTAATAAAAAAAAAAAGGAGGTGCCTAAGTACATGCCTGAGTGCGGGTTTA ACTAGAGTTCATTATTGATTAATGTGTGTACTGGACATGCCTGTTCCCAGGCAGACGGCCAAGTTCCACAGGCAGACG GCCAAGTTCCTGGGCAGTCTGCCAAGTTTCTATTTTGGACACGCGCACTTCCTGTTCCTAACCGCGGTCAGAACAAGT TAGAACAACAACCAGCCCATAACCTCTTTTTTTTTTTAAGTAAAAAAAAAAAGAAGAAAAAGAATCTTAACCCTCTGTC ATCAAATCCTGAACCTTCTAGAAGATCTACTAAAGTAAGTCTTTTTTTTTTTTAGATG
NJPyV KF954417	CATTTACCTGCCTAGAAGACCTTGCAGCCCGCAGCGAAGCAAGTAAGTGCAAGTGTGGGGCTAATTAGGTCTCTCTCCTTTTTAT AAGATTGAGGTAGAGGCAAGAGGCCTCCTGCCTCACCACAAATTAAAAAAAAAAACATCTCTATGTTTGAGCCCTCCTG ACTGGTTGCCACCAAGTCCGGGAAGGCAGCCAAGGTCAGGGCTGCCTGCCAATGTGGTTAATTATTACACTTGGGAAC CACAGGCGGCGCGTGGCTGCTCGCCAAACACAGCAGTAAATTGAAGGAAGTTGACTCTGTGTGATCATTGTGACCAG CCAGGCGAAACAGAGACACGCGACCAAACAAGAGAAAGCAAGTTACTGTTATTTCTTGTAAGTAAAACTTAATTTT TTAATTCTTTTTAGAATG

[a]NCCR sequences were retrieved from the GenBank database, chemically synthesized, and inserted into the bidirectional reporter vector (see Materials and Methods).

LTag and was now located among those HPyVs conferring NCCR-driven EVGR expression equal to or higher than that of BKPyV. Compared to HEK293, EVGR expression in HEK293T cells increased more than 10-fold for some HPyV NCCRs, including BKPyV, whereas only little change was observed for HPyV6. LVGR expression also increased but to a lesser extent (Fig. 3C). Thus, most, but not all HPyV NCCRs were able to respond to SV40 LTag in *trans* with significantly increased EVGR expression.

As noted above, the LTag-binding sites differed in number and location among the different HPyV NCCRs (Fig. 1). HPyV6 and HPyV7 NCCRs contained the lowest numbers

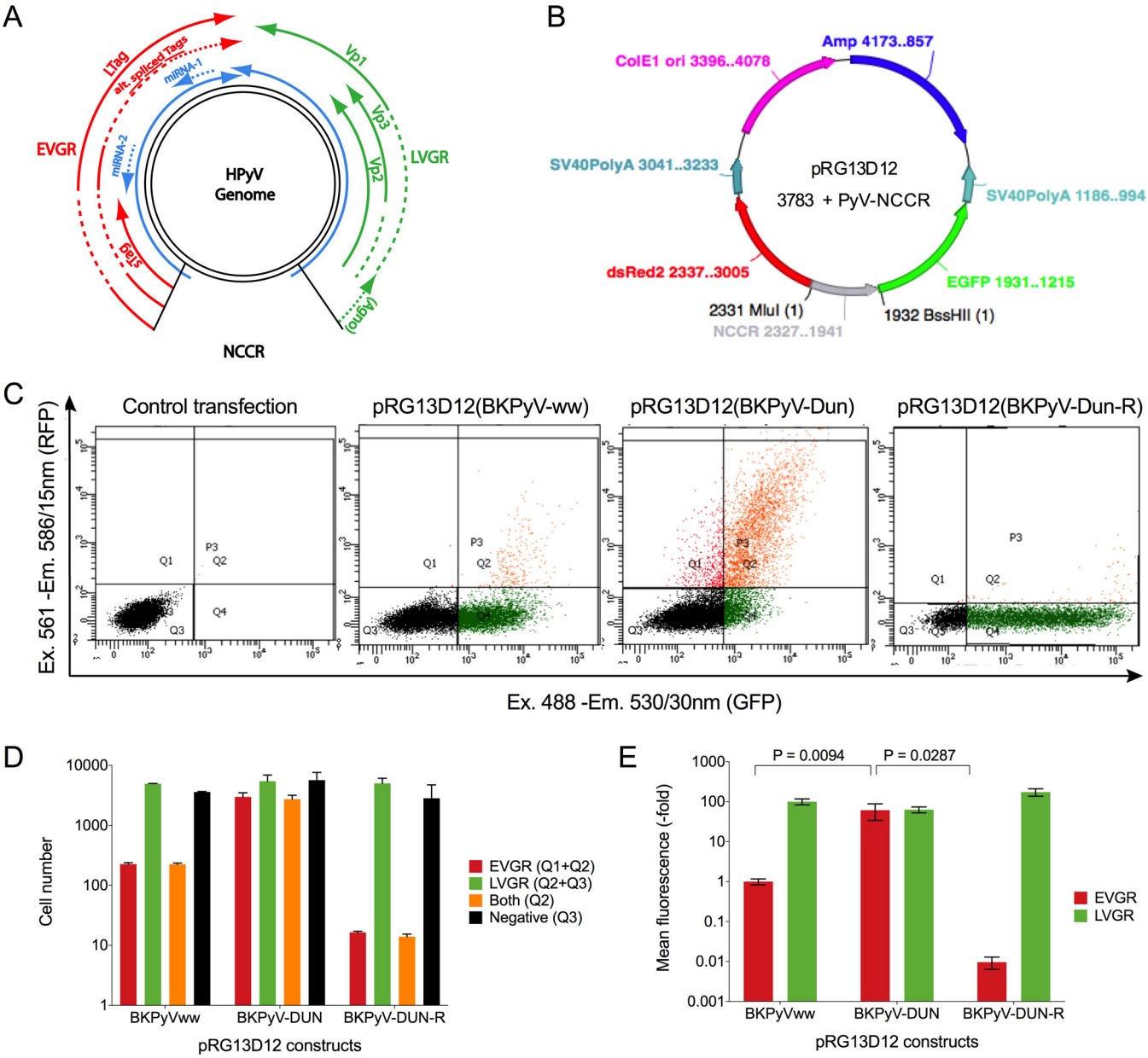

FIG 2 Rearranged BKPyV Dunlop NCCR showed higher EVGR expression than did BKPyVww NCCR in HEK293 cells. (A) Schematic representation of the HPyV genome: noncoding control region (NCCR); early viral gene region (EVGR, in red) encoding large and small T antigens (Tags), alternative spliced Tags; microRNAs (blue arrow); late viral gene region (LVGR) encoding structural proteins (Vp1, Vp2, and Vp3) and the agnoprotein (agno) only in BKPyV and JCPyV. (B) Representation of the bidirectional reporter vector pRG13D12, containing the following: NCCR (in gray) in the early to late orientation cloned via restriction sites MluI and BssHII; the red fluorescence protein dsRed2, used as a marker of EVGR expression; the enhanced green fluorescence protein, EGFP, in the opposite orientation, used as a marker of LVGR expression; SV40 polyadenylation signals [SV40 poly(A)] for the dsRed2 and EGFP expression cassette; E1 ori for bacterial plasmid replication; the ampicillin-resistant gene (Amp) for selecting *Escherichia coli* transformants. (C) Flow cytometry of HEK293 cells 2 dpt with the pRG13D12 reporter vector alone or containing the NCCR of the archetype BKPyVww, the BKPyV(DUN), or the BKPyV(DUN-R) in the reverse orientation. *x* axis, EGFP fluorescence; *y* axis, dsRed2 fluorescence; 10,000 control transfected cells were gated for the live gate, while 5,000 transfected cells were gated for the P3 (Q1, Q2, and Q4) gate. Q1, Q4, and Q2 depict cells expressing red fluorescence, green fluorescence, and both, respectively. Ex, excitation wavelength; Em, emission wavelength. (D) Quantification of cells: red bars, sum of red cells (Q1 + Q2); green bars, sum of green cells (Q2 + Q4); yellow bars, red- and green-fluorescence double-positive cells (Q2); black bars, nonfluorescent cells (Q3, negative). Means with standard deviations (SD) from three independent replicates are shown. (E) Normalized mean fluorescence intensity (MFI). The weighted MFI was calculated for each measurement (see formulas in Materials and Methods); late expression was normalized to BKPyVww NCCR (green MFI was set as 100), while early expression was normalized to BKPyVww NCCR (red MFI was set as 1). Means with SD from three independent replicates are shown.

(1 and 2 sites, respectively) of LTag-binding sites, while MCPyV NCCR harbors the highest number (12 sites) of LTag-binding sites, which appeared to partly correlate with the EVGR expression levels in HEK293T cells (Spearman's correlation, $r = 0.625$; $P < 0.05$) (Fig. 3D). Of note, HPyV12 and TSPyV deviated by showing significantly higher and

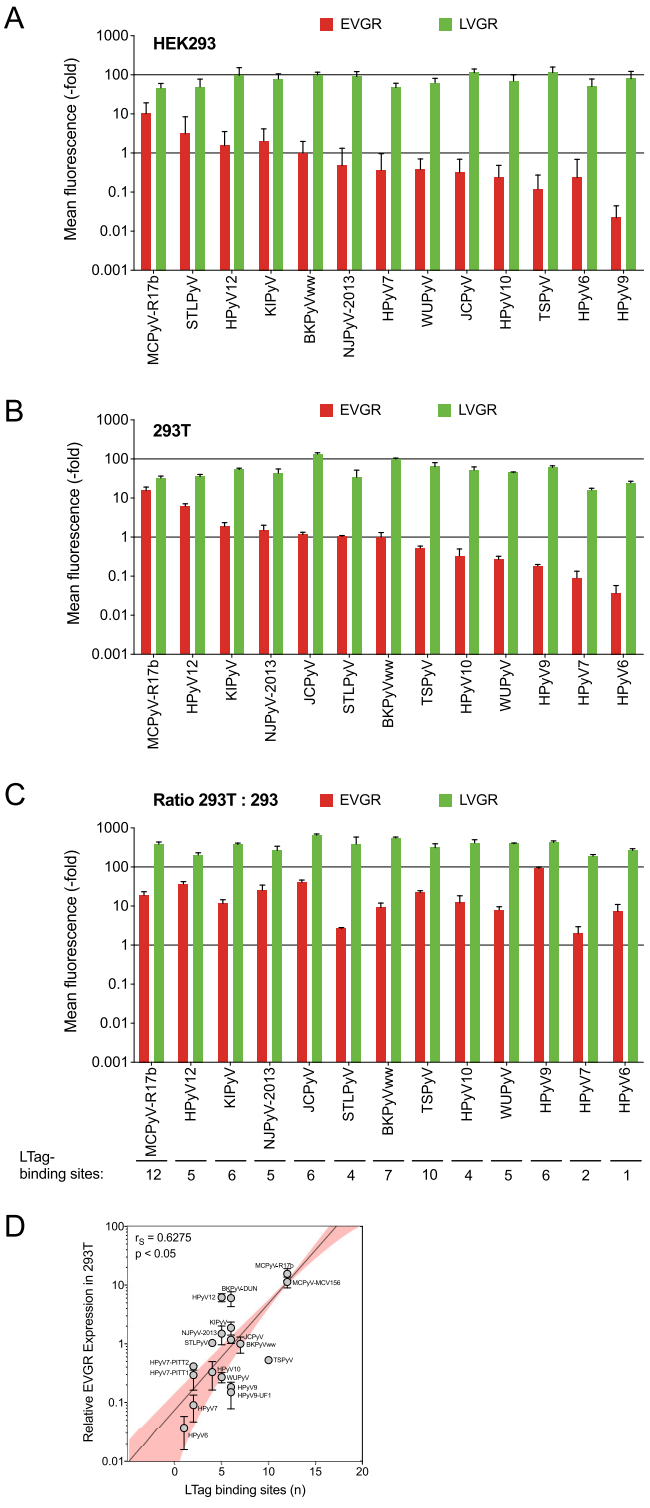

FIG 3 HPyV NCCRs differ in EVGR expression in HEK293 and 293T cell lines. (A) HEK293 normalized to archetype BKPyV(ww) (error bars indicate SD); (B) HEK293T cells normalized to archetype BKPyV(ww) (error bars indicate SD); (C) fold changes in 293T versus HEK293 cells (error bars indicate SD from three independent replicates); (D) log-linear regression (*y* axis, log; *x* axis, linear; 95% confidence interval shown in pink) of LTag-binding sites and EVGR expression in 293T cells.

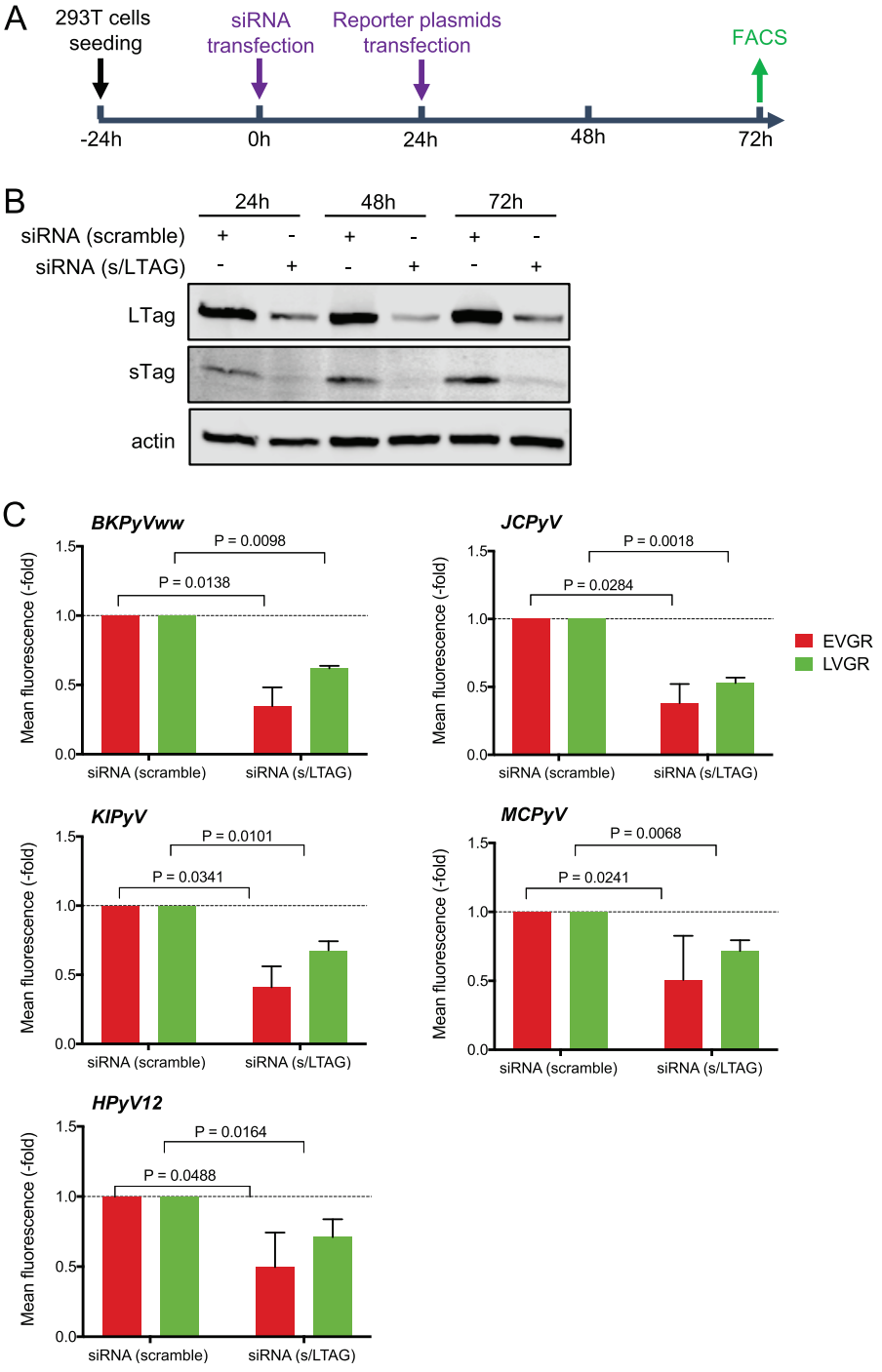

FIG 4 siRNA knockdown of SV40-sT/LTag expression in 293T cells. (A) Experimental timeline of transfection and flow-cytometric analysis (fluorescence-activated cell sorter [FACS]). (B) Immunoblot demonstrating efficient knockdown of LTag protein and sTag protein in 293T cells transfected with siRNA (sT/LTAG or scrambled) for up to 72 h. Immunoblotting against the actin protein was used as a loading control. (C) Mean fluorescence intensity of the indicated NCCR reporter constructs.

lower levels, respectively, than the others. To ensure a significant role of SV40 Tag expression in the observed increase in NCCR gene expression, 293T cells were first transfected with small interfering RNA (siRNA) targeting a common sequence of the sTag and LTag transcripts, and the results of sTag and LTag protein levels and corresponding bidirectional reporter gene expression were compared to those obtained with control cells transfected with scrambled siRNA (Fig. 4). As shown for the

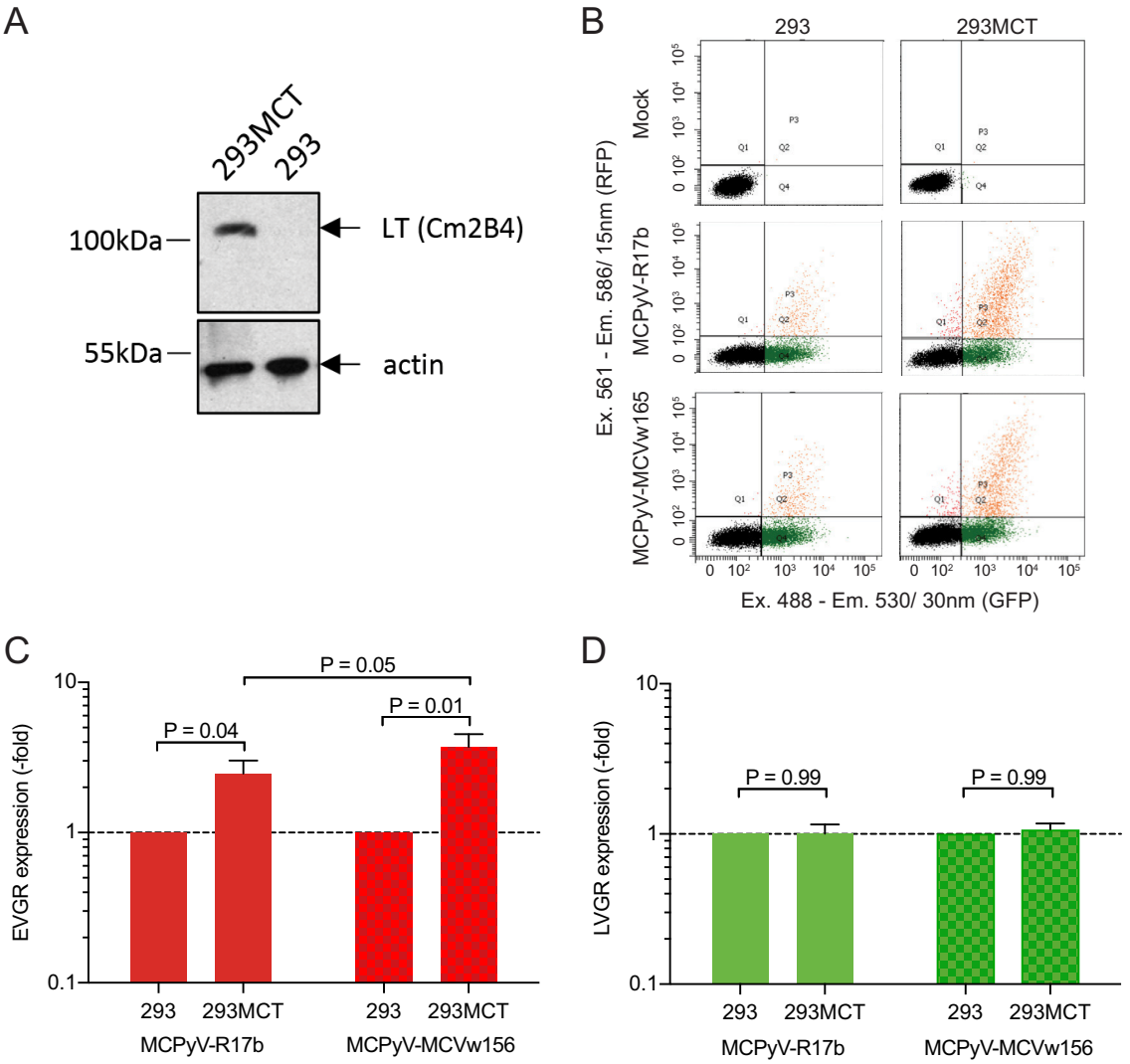

FIG 5 MCPyV NCCR response in MVPyV T antigen-expressing 293MCT. (A) MCPyV LTag expression in 293MCT cells (immunoblot); (B) Flow cytometry of MCPyV-17b and MCPyV-MCVw156; (C) EVGR expression presented as fold changes in HEK293 cells; (D) LVGR expression expressed as fold changes in HEK293 cells. Means with SD from three independent replicates are shown; the Wilcoxon *t* test was used.

NCCRs of BKPyV, JCPyV, KIPyV, MCPyV, and HPyV12, reporter gene expression at 72 hpt was reversed by the s/LTag siRNA. Together, the data indicated that SV40 LTag in *trans* provided an important stimulus to the basal EVGR expression of most HPyV EVGRs but also suggested that other factors related to the primary HPyV NCCR sequence mattered.

Autologous MCPyV LTag increases MCPyV NCCR EVGR expression. Although SV40 LTag has considerable homology to the LTag encoded by HPyV genomes (32, 33), differences in amino acids and in the host range domain have been noted, which can be grouped in one of seven clades (51). We wondered whether or not the known strong and pleiotropic action of SV40 LTag in 293T cells could be an appropriate indicator and surrogate of the cognate viral LTag. We addressed this question for MCPyV by examining two MCPyV NCCR reporter constructs in 293MCT cells (52) expressing the cognate MCPyV LTag (Fig. 5A). One NCCR had been detected in healthy skin and was tested previously (MCPyV-R17b) (9), while the other one had been detected in a Merkel cell carcinoma carrying 1 C→G substitution and 1 A base deletion in an A-rich sequence stretch (MCPyV-MCVw156) (53). The results demonstrated increased EVGR expression from two different MCPyV NCCRs in 293MCT cells, thus independently supporting the results obtained with SV40 LTag in 293T cells (Fig. 5B, C, and D).

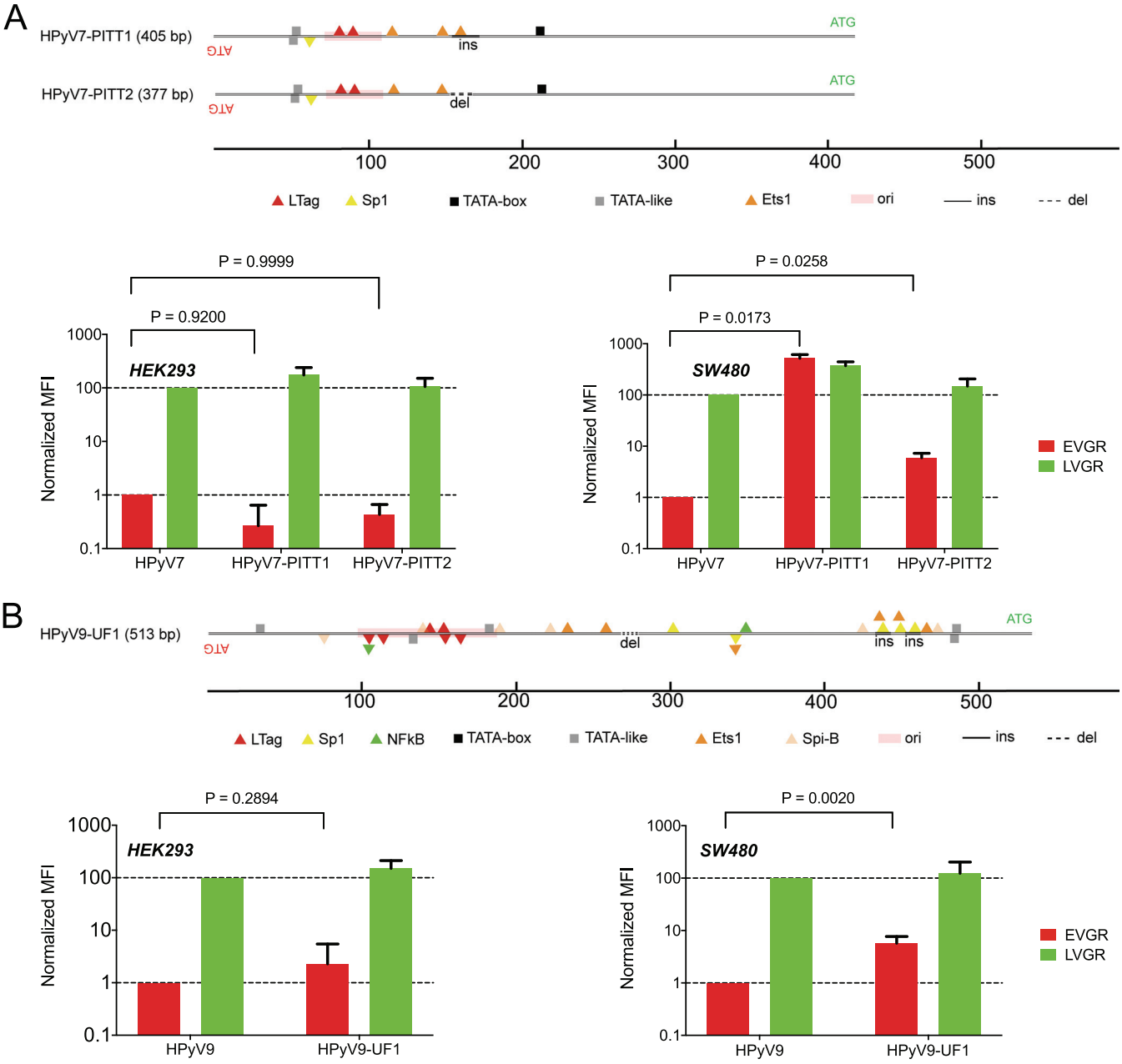

FIG 6 Clinical NCCR rearrangements of HPyV7 and HPyV9. (A) HPyV7-PITT1 carries a 16-bp insertion (ins); HPyV7-PITT2 carries a 12-bp deletion (del, dotted line) compared to the archetype HPyV7 NCCR shown in Fig. 1. EVGR and LVGR expression shown as fold changes in HEK293 or SW480 cells, respectively. Means with SD from three independent replicates are shown; the Wilcoxon *t* test was used. (B) HPyV9-UF1 carries an insertion providing 3 additional Sp1 sites compared to archetype HPyV7 shown in Fig. 1. EVGR and LVGR expression shown as fold changes in HEK293 and A549 cells, respectively. Means with SD from three independent replicates are shown; the Wilcoxon *t* test was used.

Rearranged NCCR patient variants increase EVGR expression. Clinical NCCR sequence variants of the novel HPyVs have been described (24, 31, 54), but their effects on bidirectional EVGR and LVGR expression have not been compared with the respective archetype NCCRs. We therefore examined the rearranged HPyV7 NCCR variants PITT1 and PITT2 (Fig. 6A) detected in two lung transplant patients with pruritic hyperproliferative keratinopathy (24). The data demonstrated a significant increase of HPyV7 PITT1 and PITT2 EVGR expression in the colon cell line SW480, while only a trend to higher levels was observed in HEK293 (Fig. 6A). For the rearranged HPyV9-UF1 (Fig. 6B), higher EVGR expression over archetype HPyV9 NCCR activity was observed in HEK293 and in the lung cancer line A549 (Fig. 6B). These results indicated that naturally

occurring NCCR rearrangements of the novel HPyV7 and -9 were able to confer increased EVGR expression but that this effect also depended on the host cell context.

Role of host cells for bidirectional NCCR expression. Given the role of the host cell context suggested above, we analyzed the NCCR-driven EVGR and LVGR expressions of the 13 HPyV NCCR reporter constructs in different cell lines derived from skin, lung, cervix, brain, and colon (Tables 2 and 3). Indeed, HPyV NCCR showed differences in EVGR and LVGR expression according to the host cell lines tested (Table 2). Thus, MCPyV demonstrated the strongest EVGR expression in the skin-derived A375 cells and intermediate levels in the epithelial cell lines derived from kidney and colon, whereas cervix, lung, and brain cell lines showed rather low EVGR expression. HPyV12 NCCR conferred the strongest expression in brain and colon, followed by lung, cervix, and skin cell lines, while remaining relatively low in kidney-derived cell lines. JCPyV NCCR EVGR expression was highest in brain-derived cells, whereas BKPyV NCCR showed the highest EVGR expression in kidney, followed by lung- and colon-derived cell lines. KIPyV NCCR-driven EVGR expression was highest in cervix and brain followed by lung, while WUPyV NCCR was highest in the colon-derived cell line (Table 2). Complementary LVGR expression levels were observed for these HPyV NCCRs, some of which decreased as the EVGR expression levels were higher. Taken together, the data demonstrate that the bidirectional activity of a given HPyV can substantially differ in different host cells.

To investigate whether or not expression of SV40 LTag in *trans* would be able to further increase the host cell-specific expression levels, A375 skin and SW480 colon-derived cells were transfected with a corresponding LTag expression vector, pRcCMV-SLT or pSG-largeT (data not shown). The results indicated that MCPyV NCCR-driven EVGR expression was significantly increased in both cell lines expressing SV40 LTag, whereas no significant changes were observed for HPyV12 NCCR-driven reporter gene expression (Fig. 7).

DISCUSSION

The results of the present study demonstrate that HPyV NCCRs not only differ in sequence length, number, and position of binding sites for LTag and rather common factors like Sp1, NF1, and Ets1 (Fig. 1) but also confer significant differences in viral gene expression. This difference in basal EVGR expression is most impressively captured in HEK293 cells by the high levels seen for MCPyV and HPyV12 NCCRs at the upper end, and which range to the 2-orders-of-magnitude-lower levels seen for HPyV6, HPyV7, and HPyV9 NCCRs. LVGR expression was generally strong but varied less among the different archetype HPyV NCCRs as described for the archetype BKPyV NCCR(ww) (34, 36).

The functionality of the bidirectional HPyV NCCR reporter activity was further addressed by providing the SV40 homolog of the EVGR-encoded LTag in *trans* (32, 55) in 293T cells, which showed increased EVGR expression levels for practically all HPyV NCCRs. This indicates that the reporter construct recapitulated an essential NCCR response described in detail for the viral life cycle of polyomavirus representatives such as SV40 or BKPyV (1, 32, 34, 47). LVGR expression was also increased, although to a lesser extent, in line with the bidirectional balance of EVGR versus LVGR expression (49). Knockdown of SV40 Tag following siRNA transfection of 293T resulted in decreased LTag expression and lowered reporter gene expression, indicating that LTag played a significant role rather than undefined clonal cell variation. Although SV40 LTag has been recognized and exploited as a strong pleiotropic activator of HPyV gene expression, the autologous LTag of some HPyVs might confer only selective responses, as reported for the JCPyV LTag and its cognate JCPyV NCCR, which are not seen for BKPyV NCCR (56). We could not assess the specific impact of each of the 13 HPyV LTag orthologues on their respective NCCRs, but our observations were supported by the impact of MCPyV LTag on 293MCT cells (52) demonstrating a similar activation of EVGR expression for two different MCPyV NCCRs, one from a healthy control and one from a Merkel cell carcinoma bearing a G-to-C point mutation.

TABLE 2 EVGR and LVGR expression of 13 HPyV NCCRs[a]

EVGR

	Transfected cell lines							
	Kidney	Kidney	Kidney	Skin	Lung	Cervix	Brain	Colon
NCCR constructs	HEK293	HEK293T	HEK293TT	A375	A549	HeLa NT	HS683	SW480
BKPyVww-E (Ab. MFI)	*49.6 (10.7)*	*553.5 (87.4)*	*136.1 (12.1)*	*10.1 (6.0)*	*19.4 (7.3)*	*2.0 (0.5)*	*7.6 (3.6)*	*13.6 (1.1)*
BKPyVww-E	1 (0.2)	1.0 (0.4)	1.0 (0.2)	1.0 (0.7)	1.0 (0.4)	1.0 (0.3)	1.0 (0.5)	1.0 (0.1)
JCPyV-E	0.3 (0.2)	1.2 (0.2)	2.5 (0.7)	0.2 (0.1)	0.9 (0.3)	4.1 (1.6)	5.0 (4.8)	3.7 (0.4)
KIPyV-E	1.5 (0.9)	1.9 (0.5)	4.9 (2.6)	3.6 (0.6)	7.0 (1.4)	31.0 (5.0)	5.5 (3.1.0)	0.6 (0.02)
WUPyV-E	0.3 (0.1)	0.3 (0.1)	0.2 (0.1)	2.5 (1.0)	1.4 (0.7)	4.7 (0.7)	2.5 (1.6)	17.3 (12.3)
MCPyV-E	7.5 (3.2)	15.6 (3.5)	12.9 (2.4)	60.6 (15.1)	0.6 (0.1)	2.1 (0.7)	2.1 (0.5)	5.5 (2.4)
HPyV6-E	0.04 (0.01)	0.04 (0.02)	0.1 (0.1)	0.7 (0.4)	0.1 (0.03)	0.1 (0.1)	0.2 (0.2)	0.2 (0.1)
HPyV7-E	0.4 (0.4)	0.1 (0.04)	0.3 (0.3)	0.6 (0.4)	0.1 (0.1)	0.5 (0.6)	2.5 (1.2)	0.2 (0.1)
TSPyV-E	0.2 (0.1)	0.5 (0.1)	0.4 (0.5)	2.0 (0.4)	0.9 (0.2)	0.5 (0.1)	1.0 (0.7)	0.2 (0.1)
HPyV9-E	0.02 (0.01)	0.2 (0.2)	1.1 (0.4)	0.4 (0.1)	0.3 (0.1)	0.4 (0.2)	2.7 (1.7)	10.6 (2.3)
HPyV10-E	0.3 (0.3)	0.3 (0.2)	0.9 (0.5)	0.4 (0.1)	1.3 (0.2)	5.9 (0.1)	2.8 (0.3)	7.8 (4.8)
STLPyV-E	3.6 (3.2)	1.0 (0.2)	3.7 (2.2)	1.7 (0.3)	0.8 (0.2)	1.6 (0.02)	0.6 (0.1)	0.3 (0.1)
HPyV12-E	1.5 (0.9)	6.2 (1.0)	11.1 (7.9)	21.3 (7.2)	22.2 (8.2)	22.1 (4.5)	37.3 (19.0)	31.0 (12.8)
NJPyV-E	0.5 (0.5)	1.5 (0.5)	1.4 (0.6)	0.7 (0.3)	3.6 (2.5)	0.2 (0.2)	0.9 (0.5)	0.5 (0.2)

LVGR

NCCR constructs	HEK293	HEK293T	HEK293TT	A375	A549	HeLa NT	HS683	SW480
BKPyVww-L (Ab. MFI)	*2883.7 (494.6)*	*15950.3 (844)*	*22727 (1356.1)*	*3372.7 (784.0)*	*4005.2 (1166.1)*	*2049.0 (12.7)*	*4112.0 (37.2)*	*5202.8 (1343.8)*
BKPyVww-L	100.0 (17.1)	100.0 (5.4)	100.0 (6.7)	100.0 (23.0)	100.0 (29.1)	100.0 (0.6)	100.0 (0.9)	100.0 (25.0)
JCPyV-L	113.6 (27.1)	134.1 (11.3)	178.3 (36.8)	102.0 (12.2)	106.5 (9.6)	111.8 (26.0)	122.7 (32.5)	127.5 (10.6)
KIPyV-L	77.7 (26.9)	53.5 (4.6)	65.7 (5.6)	68.3 (3.6	72.2 (2.8)	173.2 (15.1)	83.2 (22.0)	83.1 (2.9)
WUPyV-L	62.8 (18.5)	44.9 (4.1)	26.7 (3.4)	64.3 (6.4)	97.3 (25.0)	188.03 (28.1)	104.9 (13.9)	95.7 (24.0)
MCPyV-L	46.3 (14.0)	32.3 (4.2)	38.4 (4.1)	40.3 (5.7)	44.1 (3.4)	74.0 (14.5)	44.8 (2.6)	55.7 (9.1)
HPyV6-L	50.6 (27.6)	24.5 (2.4)	29.0 (2.4)	13.8 (1.1)	29.0 (4.6)	79.8 (22.0)	32.9 (17.3)	47.1 (9.5)
HPyV7-L	47.3 (13.4)	16.2 (1.6)	19.2 (1.6)	13.2 (0.9)	22.7 (1.7)	44.0 (4.0)	27.2 (5.4)	34.5 (6.84)
TSPyV-L	113.2 (45.2)	63.7 (16.6)	78.8 (16.5)	83.9 (19.5)	99.3 (16.6)	159.0 (16.0)	120.0 (14.3)	144.0 (14.47)
HPyV9-L	79.4 (48.0)	61.2 (5.6)	74.2 (5.8)	23.8 (3.7)	21.8 (4.1)	70.6 (13.3)	32.3 (8.2)	41.4 (17.4)
HPyV10-L	69.4 (31.7)	51.9 (10.7)	61.8 (10.5)	23.3 (3.6)	54.3 (3.0)	51.6 (4.8)	62.5 (10.8)	50.4 (7.2)
STLPyV-L	49.0 (28.6)	34.0 (4.1)	39.7 (17.3)	12.1 (2.7)	21.1 (2.4)	33.1 (3.2)	23.8 (10.2)	48.3 (5.4)
HPyV12-L	96.2 (42.3)	34.1 (17.6)	44.0 (5.5)	74.0 (7.3)	137.2 (38.1)	150.0 (21.4)	102.6 (19.0)	100.9 (4.8)
NJPyV-L	90.0 (30.4)	43.6 (11.8)	55.2 (13.0)	19.8 (4.8)	78.7 (8.7)	71.8 (18.0)	86.8 (15.9)	66.0 (10.4)

[a]The indicated HPyV NCCR reporter plasmids were transfected in the indicated cell lines. Red and green fluorescence levels were measured by flow cytometry and normalized using BKPyV-NCCR(ww) as the reference, with BKPyV EVGR as 1 and BKPyV LVGR as 100 (SD) as detailed in Materials and Methods.

The role of the HPyV NCCR sequences as differential determinants of EVGR and LVGR expression was further strengthened by the correlation of the number of LTag-binding sites and the level of EVGR expression in 293T cells. However, there were also two notable exceptions, such as HPyV12 NCCR, which showed much higher EVGR expression than predicted from the number of LTag-binding sites, whereas the opposite was true for the TSPyV NCCR EVGR response. This suggested that other regulatory elements were critical in determining the EVGR response. In this analysis, the higher expression of rearranged BKPyV(DUN) NCCR compared to the archetype BKPyVww should be noted, in which one LTag site is deleted together with the high-affinity *SP1-4* site in the LVGR promoter (49). Deletions and insertions in HPyV7 PITT1, HPyV PITT2, and HPyV9 UF1 were also associated with increased EVGR expression despite rather small alterations of the primary sequence. Thus, HPyV NCCR sequences are key determinants of

TABLE 3 Cell lines transfected with NCCR reporter constructs

Cell line	Culture medium (supplemented with 10% FBS, 2 mM glutamine)	Transfection reagents	Origin	Cell line source
HEK293	DMEM-H	Lipofectamine 2000	Human embryonic kidney cells	ATCC CRL-1573
HEK293T	DMEM-H	Lipofectamine 2000	Human embryonic kidney cells expressing SV40 LTag and sTag	ATCC CRL-3216
HEK293TT	DMEM-H plus 400 μg/ml hygromycin B	Lipofectamine 2000	Human embryonic kidney cells expressing SV40 LTag and sTag	NCI-Frederick Repository Service, Frederick, MD, USA
HEK293MCT	DMEM-H	Lipofectamine 2000	Human embryonic kidney cells expressing MCPyV LTag and sTag	Gift from Nicole Fischer from Institute for Microbiology and Virology, University Medical Center Eppendorf, Hamburg, Germany
A375	DMEM-H	Lipofectamine 2000	Human malignant melanoma cells	ATCC CRL-1619
A549	EMEM	Lipofectamine 3000	Human epithelial lung adenocarcinoma	ATCC CCL-185
HeLa NT	DMEM-H	Lipofectamine 2000	Human cervical carcinoma cells	Gift from Natalia Teterina from Laboratory of Viral Diseases, National Institute of Allergy and Infectious Diseases, National Institutes of Health, Bethesda, MD, USA
HS683	DMEM-H	Omni avalanche	Human brain glioma cells	ATCC HTB-138
SW480	EMEM	Lipofectamine 2000	Human colon adenocarcinoma cells	ATCC CCL-228

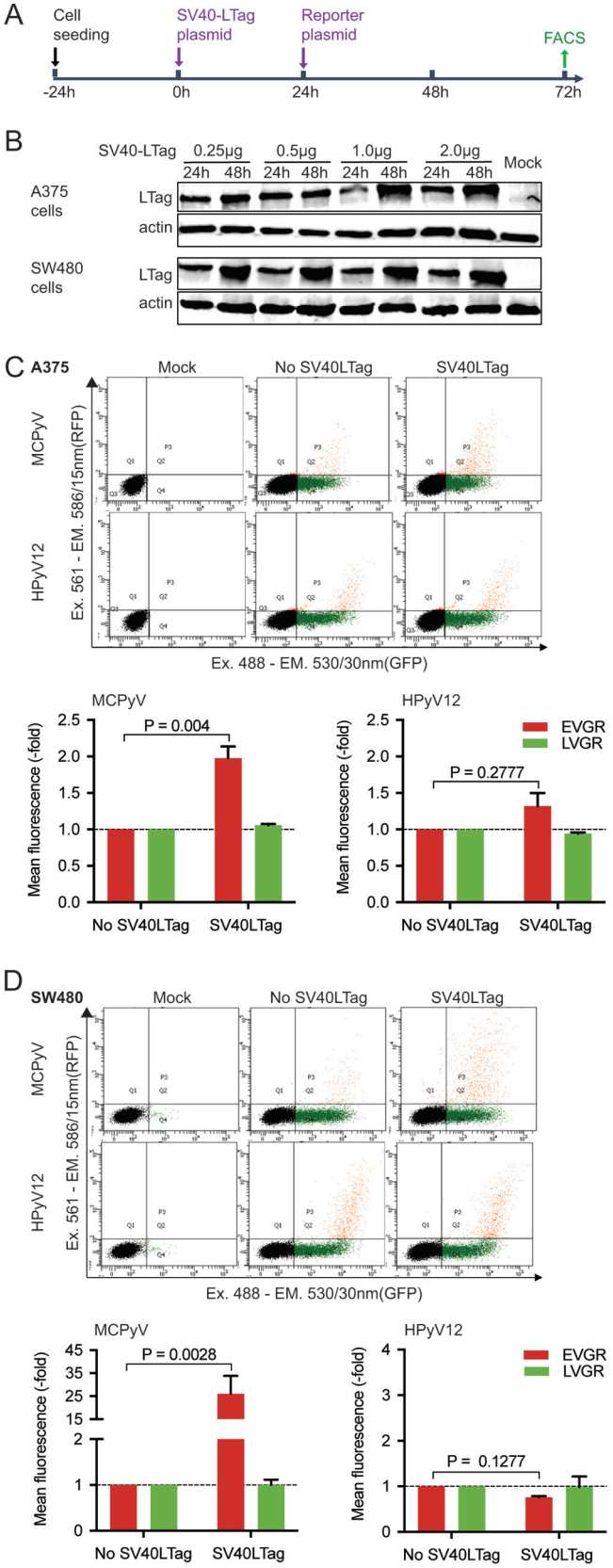

FIG 7 Effects of SV40 LTag expression on MCPyV and HPyV12 expression in A375 skin and SW480 colon cells. (A) Experimental timeline of transfection and flow cytometric analysis (FACS). (B) Immunoblot demonstrating LTag expression in A375 and SW480 cells transfected with the indicated amounts of an

(Continued on next page)

EVGR activity, and this suggests for the first time that the pathogenicity of the rearranged variants would likely be increased in susceptible host cells as shown before for clinical variants of BKPyV and JCPyV NCCRs (34, 37).

Finally, we noted that HPyV NCCR expression levels differed in different host cell lines, emphasizing that the combined cellular make-up of transcription factors and other regulatory proteins is essential in sensing and interpreting the HPyV NCCRs with respect to viral gene expression and persistence (33). Transfection of skin- and colon-derived cells with an SV40 LTag expression vectors provided evidence that MCPyV NCCR-driven EVGR expression could be further increased, most prominently in the SW480 colon-derived cells, whereas this was not the case for the HPyV12 NCCR in these cells, indicating that the NCCR and specific host cell factors may be critical also for LTag-mediated effects.

As this work was in progress, Moens and colleagues independently reported the characterization of HPyV NCCRs in different cell lines using a unidirectional luciferase reporter assay, which identified higher EVGR expression by MCPyV and HPyV12 NCCRs, similar to our results, but also for TSPyV NCCR (57), which was not seen in our study. Although unidirectional reporter assays have been commonly used, they remain challenging for a bidirectional gene expression organization within a small DNA sequence of approximately 500 bp (Fig. 1). Part of this stems from the difficulty to generate well-justified and controlled truncations of the intricately intertwined and competing functional elements of the bidirectional HPyV NCCR (47, 49), which may be difficult to accomplish given the pronounced functional effects of even single-point mutations (47). Unfortunately, their approach is also faced with the difficulty of ensuring directly equivalent transfection efficacies for each of their unidirectional assessments of the early gene expression and then again of the late gene expression (57). These caveats render a straightforward assessment of the early versus late activity difficult. Most notably, the unidirectional approach may be subject to undefined and possibly host cell-dependent effects from the direct joining of unrelated plasmid sequences, which arise from NCCR truncation on the opposite end of the reporter gene. Experimental studies of the SV40 NCCR have shown that unrelated sequences can have substantial effects on NCCR function (58, 59). This may be responsible for some of the discrepancies between the unidirectional approach and the more-physiological bidirectional approach used by us. Among others, Moens et al. reported the highest MCPyV-EVGR expression in the colon cell line (SW480), whereas we observed the highest expression level in skin-derived A375 cells (57). Moreover, we demonstrate that the lower levels of MCPyV-EVGR expression in the colon cell line (SW480) could be further increased by LTag expression. Together with our previous analyses (34, 37), we are confident that the bidirectional reporter assays used here recapitulates the physiological HPyV NCCR organization and activity, which can be robustly enumerated in single cells using flow cytometry and includes estimates of nontransfected nonfluorescent cells (47, 49).

Our comprehensive analysis of the bidirectional HPyV NCCR reporter expression using flow cytometry also provides estimates for different model cell lines derived from kidney, skin, lung, cervix, colon, and brain. The results suggest that there may be underlying mechanisms linked to cell differentiation and the respective HPyV NCCR as expected for a coevolutionary relationship. Thus, EVGR expression of MCPyV NCCR was

FIG 7 Legend (Continued)
SV40 LTag expression construct or mock control. Equal protein amounts per lane were ensured by immunoblotting against actin. (C) Flow cytometry analysis of A375 skin cells after transfection of SV40 LTag expression vector and the bidirectional reporter vector containing the MCPyV NCCR or the HPyV12 NCCR, respectively. Upper panels show a representative example; lower panels show mean fluorescence intensity of RFP (early region) and GFP (late region) of MCPyV and HPyV12 NCCR reporter constructs in A375 cells. (D) Flow cytometry analysis of SW480 colon cells after transfection of SV40 LTag expression vector and the bidirectional reporter vector containing the MCPyV NCCR and the HPyV12 NCCR, respectively. Upper panels show a representative example; lower panels show mean fluorescence intensity of RFP (early region) and GFP (late region) of MCPyV and HPyV12 NCCR reporter constructs in SW480 cells.

even stronger in skin-derived cell line A375 than in the kidney-derived reference HEK293 or 293T derivative cell line, whereas that of BKPyV NCCR was strongest in kidney-derived, and that of WUPyV in colon-derived, cell lines (Table 1). Although identifying these promoting or restricting factors in the respective cell lines requires further study, their nonrandom viral expression profile is intriguing and suggests a first functional characterization of secondary HPyV host cell tropism through this bidirectional reporter assay. The combination of host cell and HPyV NCCR reporter vector should be amenable to molecular screening approaches using loss-of-function approaches, e.g., through short hairpin RNA (shRNA) knockdown libraries as reported previously (48), or gain-of-function approaches, e.g., through expression library or corresponding small-compound libraries. Clearly, our correlation of functional response and NCCR sequence does not presently allow to simply delineate candidate sequences or factors but requires further fine mapping as done for the BKPyV NCCR (47). In this regard, the current lack of straightforward HPyV culture and replication models must be acknowledged as a limitation. This obstacle is somewhat at odds with the rather frequent detection of certain HPyVs such as HPyV6 and HPyV7 on healthy skin and the rather poor NCCR expression levels observed here as well as by others, which suggests that important host cell factors must be identified before cell culture work can be successful.

The high number of HPyVs in humans continues to surprise (60), as comprehensive serological studies using specific Vp1-based IgG detection indicate that most humans have been infected with more than one (17–19, 61). On average, 6 to 7 HPyV coinfections are present (19), some which may coexist in the same organ as shown for skin and kidney and may show direct positive and negative viral interactions (60).

In summary, HPyV NCCRs mediate key functions of polyomavirus biology, including the persistence of the episomal viral genome in the host cell nucleus as well as timing and sequential steps of the viral replication cycle. Despite some limitations, our results are informative and represent an important step toward understanding secondary HPyV cell tropism beyond HPyV surface receptors. By identifying key viral and host factors shaping the viral life cycle, models of HPyV infection, replication, and disease can be developed to identify suitable antiviral targets.

MATERIALS AND METHODS

HPyV NCCR and reporter constructs. Based on the phRG1 reporter vector (34) recapitulating the principal HPyV genome organization with respect to EVGR and LVGR (Fig. 2A), a smaller bidirectional reporter, pRG13D12, was constructed, in which the expression cassette for hygromycin resistance was removed, and the reporter genes were placed upstream of SV40 polyadenylation sites instead of those from beta-globin (Fig. 2B). The HPyV NCCRs were chemically synthesized in pUC57 (Eurogentec S.A, Belgium) (Table 1), excised using the restriction enzymes BssHII and MluI (New England BioLabs, England), and cloned into the corresponding restriction sites of pRG13D12. HPyV NCCR constructs were verified by Sanger sequencing for correct NCCR sequences and orientations using the 3130 genetic analyzer (Applied Biosystems, Switzerland). The SV40 LTag expression vector pSG-largeT was obtained from AddGene, the pRcCMV-SLT (62) was kindly provided by Ugo Moens, University of Tromso, Norway, and both were transfected using Lipofectamine 2000 as described below.

Cell lines. The cell lines, their origin and providers, and the standard culture conditions are listed in Table 2. All cell lines were cultured in a HERA cell-150 incubator (ThermoFisher Scientific, Switzerland) at a temperature of 37°C and 5% CO_2.

siRNA knockdown. siRNA for SV40 LTag, 5′-AAAATTGTGTACCTTTAGCTT-3′ (63), and a scramble control siRNA were synthesized (Eurogentec S.A, Belgium). To determine the effects of siRNA transfection, 1.5×10^5 HEK293T cells were seeded in 12-well plates and transfected 24 h postseeding with 30 nM siRNAs using Lipofectamine 2000 according to the manufacturer's instructions. After 24, 48, and 72 hpt, cells were harvested for SV40 LTag and sTag immunoblotting. To analyze the effect of LTag knockdown on reporter expression, reporter plasmids were transfected at 24 h post-siRNA transfection.

Plasmid DNA transfection. Cell transfection was done in a ratio of 1:3 DNA to transfection reagent using 3 μl Lipofectamine 2000 (Thermo Fisher Scientific) and 1 μg plasmid construct in a 12-well plate, except for SW480 cells, which were transfected with 3 μl Lipofectamine 3000 (Thermo Fisher Scientific) and 1 μg plasmid constructs. For each well, 3 μl of Lipofectamine 2000 (or Lipofectamine 3000) was diluted in 100 μl of Opti-MEM (Thermo Fisher Scientific) medium, flicked, spun down, and incubated at room temperature (RT) for 5 min. One microgram of plasmid DNA was diluted in 100 μl of Opti-MEM medium for each well. Transfection reagents and plasmid DNA were then mixed, incubated for 5 min at RT, and added to the cells with a confluence ranging between 70 and 90%. Twenty-four hours posttransfection (hpt), medium was replaced with Dulbecco's modified Eagle medium (DMEM) with 10%

fetal bovine serum (FBS) or DMEM high glucose (DMEM-H) with 10% FBS complemented with 2 mM glutamine. Forty-eight hours posttransfection, fluorescence images were taken by fluorescence microscopy and EVGR (red fluorescence protein [RFP]) and LVGR (green fluorescent protein [GFP]) expressions were quantified by flow cytometry.

Immunoblotting. Cells were lysed in triple-buffer (50 mM Tris-HCl [pH 8.0], 150 mM NaCl, 1% sodium deoxycholate [NaDOC], 1% Triton X-100, and 0.1% SDS) containing 1× protease inhibitors (Roche). Equal volumes of 20 μg of cell lysates were separated by SDS-PAGE (Serva, GmbH) using running buffer (50 mM Tris base, 199 mM glycine, 0.1% SDS, pH 8.3) at 25 mA/gel for 50 min. The proteins were then electrotransferred (semidry method) onto a 0.45-μm polyvinylidene difluoride (PVDF-FL) membrane (IPFL00010; Millipore/Merck, Darmstadt, Germany) using 1× transfer buffer (10×, consisting of 48 mM Tris base, 390 mM glycine, 10% SDS) at 70 mA/gel for 48 min. The membrane was dried, reactivated with 5 ml methanol (Sigma-Aldrich, Switzerland), and washed twice with milli-Q H_2O. Odyssey blocking buffer (927-40000; Licor, Lincoln, NE, USA) diluted 1:2 in Tris-buffered saline (TBS) was used to block the membrane at RT for 1 h. Incubation of the membrane was done with the following primary antibodies: monoclonal mouse anti-actin (1:5,000; Abcam, Cambridge, England), mouse IgG2 anti-LTag cross-reacting with sTag (1:500; BD Pharmingen), diluted in 1:2 Odyssey blocking buffer–TBS–0.1% Tween 20 at RT for 2 h. The membrane was then washed at least 5 times with TBS–0.1% Tween 20. Next, the membrane was incubated in the following secondary antibodies: donkey anti-mouse Alexa Fluor 680 (1:15,000; A10038; Invitrogen) diluted in 1:2 Odyssey blocking buffer–TBS–0.1% Tween 20 at RT for 2 h. The membrane was washed at least 3 times with TBS–0.1% Tween 20. Detection of protein was done with the Licor Odyssey CLx instrument (Licor, Homburg, Germany).

Flow cytometer-based quantification. Cells were washed once at 48 hpt with 1 ml phosphate-buffered saline (PBS)–2.5 mM EDTA (BioConcept, Switzerland) and then treated with trypsin (without phenol red)–0.25 mg/ml EDTA (Lonza, MD, USA). The cells were suspended in 1 ml DMEM (without phenol red) containing 20 mM HEPES, 2 mM glutamine, 1% FBS, and 1% penicillin-streptomycin (P/S) (Thermo Fisher Scientific, Switzerland) and transferred to 5-ml polystyrene round-bottom tubes (BD, Franklin Lakes, NJ, USA). Prior to each measurement, DAPI (4′,6-diamidino-2-phenylindole; D8417; Sigma-Aldrich, St. Louis, MO, USA) was added to mark dead cells in a final concentration of 1 ng/ml. A Fortessa cytometer (Becton-Dickinson, Franklin Lakes, NJ, USA) was used as follows: for RFP, excitation at 561 nm (yellow-green laser), emission at 586/15 nm; for GFP, excitation at 488 nm (blue laser), emission at 530/30 nm; for DNA staining with DAPI, excitation at 405 nm (violet laser), emission at 450/50 nm. Transfection with pUC19 was used to set the gates for nonfluorescent transfection control cells in quadrant Q3, and the cell numbers in the corresponding quadrants were determined (Q1 for red-only cells; Q2 for red and green cells; Q3 for nonfluorescent cells; Q4 for green-only cells). The numbers of fluorescence cells for red, green, and both were calculated as follows: red, number of cells in Q1 and Q2; green, number of cells in Q2 and Q4; red and green, number of cells in Q2. The mean fluorescence intensities (MFI) for EVGR (red) and LVGR (green) expression were calculated by inserting the cell number (N) and mean fluorescence (I) of the quadrants Q1 (red cells only), Q2 (red and green cells), and Q4 (green cells only) into the respective following formulas: $MFI_{(red)} = [(N_{Q1} * I_{Q1}) + (N_{Q2} * I_{Q2})]/(N_{Q1} + N_{Q2} + N_{Q4})$ and $MFI_{(green)} = [(N_{Q2} * I_{Q2}) + (N_{Q4} * I_{Q4})]/(N_{Q1} + N_{Q2} + N_{Q4})$. EVGR expression of all HPyV constructs was normalized to the EVGR (red) and LVGR (green) expressions of the archetype BKPyV NCCR(ww), set as 1 and 100%, respectively. Dot plot images from the flow cytometer were processed in Adobe Illustrator CS4 14.0.0.

LTag expression in 293 cells stably transfected with MCPyV early gene region (293MCT cells). 293 cells were transfected with 100 ng linearized plasmid DNA encoding the MCPyV early gene region. After puromycin selection, cells were lysed and analyzed by immunoblotting for MCPyV LTag expression using the mouse monoclonal MCPyV LTag antibody Cm2B4. Equal protein amounts loaded (30 μg) were ensured by reincubating the membrane with an anti-actin antibody (Chemicon catalog number 1501) (lower blot). Parental cell line 293, negative for MCPyV LTag expression, was used as a control on the immunoblot.

***In silico* analysis of HPyV NCCRs.** The MatInspector software tool (Genomatix, Munich, Germany) (50) was used to search for potential transcription factor- and LTag-binding sites within the HPyV NCCR. The NCCR sequences were uploaded into the MatInspector software tool using the settings described for BKPyV (49). For the identification of potential LTag-binding sites, the consensus sequence GRGGC (where R is A or G) was used, allowing no mismatch.

Statistics. The means and standard deviations (SD) were calculated from three independent transfections using Microsoft Office Excel for Mac 2011 and GraphPad Prism software (version 7.0c for Mac OS). Multiple-comparison 2-way analysis of variance (ANOVA) was used for calculating the statistical differences between NCCR reporters construct expression in different cell lines and 2-way comparisons as appropriate. Correlation analysis was done by the nonparametric Wilcoxon test or log-linear Spearman regression.

ACKNOWLEDGMENTS

This research was supported by an appointment grant of the University of Basel to H.H.H. The funders played no role in the choice of topic or in the results or interpretation of the study or in the writing of the manuscript.

We thank Ugo Moens, University of Tromso, Norway, for providing the SV40 LTag expression vector pRcCMV-SLT.

REFERENCES

1. DeCaprio JA, Imperiale MJ, Major EO. 2013. Polyomaviruses, p 1633–1661. *In* Knipe DM, Howley P, Cohen JI, Griffin DE, Lamb RA, Martin MA, Racaniello VR, Roizman B (ed), Fields virology, 6th ed. Lippincott Williams & Wilkins, Philadelphia, PA.
2. Polyomaviridae Study Group of the International Committee on Taxonomy of Viruses, Calvignac-Spencer S, Feltkamp MC, Daugherty MD, Moens U, Ramqvist T, Johne R, Ehlers B. 2016. A taxonomy update for the family Polyomaviridae. Arch Virol 161:1739–1750. https://doi.org/10.1007/s00705-016-2794-y.
3. Greenlee JE, Hirsch HH. 2017. Polyomaviruses, p 599–623. *In* Richman D, Whitley R, Hayden F (ed), Clinical virology, 4th ed. ASM Press, Washington, DC. https://doi.org/10.1128/9781555819439.
4. Gardner SD, Field AM, Coleman DV, Hulme B. 1971. New human papovavirus (B.K.) isolated from urine after renal transplantation. Lancet i:1253–1257.
5. Padgett BL, Walker DL, ZuRhein GM, Eckroade RJ, Dessel BH. 1971. Cultivation of papova-like virus from human brain with progressive multifocal leucoencephalopathy. Lancet i:1257–1260.
6. Bialasiewicz S, Whiley DM, Lambert SB, Wang D, Nissen MD, Sloots TP. 2007. A newly reported human polyomavirus, KI virus, is present in the respiratory tract of Australian children. J Clin Virol 40:15–18. https://doi.org/10.1016/j.jcv.2007.07.001.
7. Gaynor AM, Nissen MD, Whiley DM, Mackay IM, Lambert SB, Wu G, Brennan DC, Storch GA, Sloots TP, Wang D. 2007. Identification of a novel polyomavirus from patients with acute respiratory tract infections. PLoS Pathog 3:e64. https://doi.org/10.1371/journal.ppat.0030064.
8. Feng H, Shuda M, Chang Y, Moore PS. 2008. Clonal integration of a polyomavirus in human Merkel cell carcinoma. Science 319:1096–1100. https://doi.org/10.1126/science.1152586.
9. Schowalter RM, Pastrana DV, Pumphrey KA, Moyer AL, Buck CB. 2010. Merkel cell polyomavirus and two previously unknown polyomaviruses are chronically shed from human skin. Cell Host Microbe 7:509–515. https://doi.org/10.1016/j.chom.2010.05.006.
10. van der Meijden E, Janssens RW, Lauber C, Bouwes Bavinck JN, Gorbalenya AE, Feltkamp MC. 2010. Discovery of a new human polyomavirus associated with trichodysplasia spinulosa in an immunocompromized patient. PLoS Pathog 6:e1001024. https://doi.org/10.1371/journal.ppat.1001024.
11. Scuda N, Hofmann J, Calvignac-Spencer S, Ruprecht K, Liman P, Kuhn J, Hengel H, Ehlers B. 2011. A novel human polyomavirus closely related to the African green monkey-derived lymphotropic polyomavirus. J Virol 85:4586–4590. https://doi.org/10.1128/JVI.02602-10.
12. Siebrasse EA, Reyes A, Lim ES, Zhao G, Mkakosya RS, Manary MJ, Gordon JI, Wang D. 2012. Identification of MW polyomavirus, a novel polyomavirus in human stool. J Virol 86:10321–10326. https://doi.org/10.1128/JVI.01210-12.
13. Lim ES, Reyes A, Antonio M, Saha D, Ikumapayi UN, Adeyemi M, Stine OC, Skelton R, Brennan DC, Mkakosya RS, Manary MJ, Gordon JI, Wang D. 2013. Discovery of STL polyomavirus, a polyomavirus of ancestral recombinant origin that encodes a unique T antigen by alternative splicing. Virology 436:295–303. https://doi.org/10.1016/j.virol.2012.12.005.
14. Korup S, Rietscher J, Calvignac-Spencer S, Trusch F, Hofmann J, Moens U, Sauer I, Voigt S, Schmuck R, Ehlers B. 2013. Identification of a novel human polyomavirus in organs of the gastrointestinal tract. PLoS One 8:e58021. https://doi.org/10.1371/journal.pone.0058021.
15. Mishra N, Pereira M, Rhodes RH, An P, Pipas JM, Jain K, Kapoor A, Briese T, Faust PL, Lipkin WI. 2014. Identification of a novel polyomavirus in a pancreatic transplant recipient with retinal blindness and vasculitic myopathy. J Infect Dis 210:1595–1599. https://doi.org/10.1093/infdis/jiu250.
16. Gheit T, Dutta S, Oliver J, Robitaille A, Hampras S, Combes JD, McKay-Chopin S, Le Calvez-Kelm F, Fenske N, Cherpelis B, Giuliano AR, Franceschi S, McKay J, Rollison DE, Tommasino M. 2017. Isolation and characterization of a novel putative human polyomavirus. Virology 506:45–54. https://doi.org/10.1016/j.virol.2017.03.007.
17. Kean JM, Rao S, Wang M, Garcea RL. 2009. Seroepidemiology of human polyomaviruses. PLoS Pathog 5:e1000363. https://doi.org/10.1371/journal.ppat.1000363.
18. Kardas P, Leboeuf C, Hirsch HH. 2015. Optimizing JC and BK polyomavirus IgG testing for seroepidemiology and patient counseling. J Clin Virol 71:28–33. https://doi.org/10.1016/j.jcv.2015.07.305.
19. Gossai A, Waterboer T, Nelson HH, Michel A, Willhauck-Fleckenstein M, Farzan SF, Hoen AG, Christensen BC, Kelsey KT, Marsit CJ, Pawlita M, Karagas MR. 2016. Seroepidemiology of human polyomaviruses in a US population. Am J Epidemiol 183:61–69. https://doi.org/10.1093/aje/kwv155.
20. Binet I, Nickeleit V, Hirsch HH, Prince O, Dalquen P, Gudat F, Mihatsch MJ, Thiel G. 1999. Polyomavirus disease under new immunosuppressive drugs: a cause of renal graft dysfunction and graft loss. Transplantation 67:918–922. https://doi.org/10.1097/00007890-199903270-00022.
21. Hirsch HH, Randhawa P. 2013. BK polyomavirus in solid organ transplantation. Am J Transplant 13(Suppl 4):179–188. https://doi.org/10.1111/ajt.12110.
22. Cesaro S, Dalianis T, Hanssen Rinaldo C, Koskenvuo M, Pegoraro A, Einsele H, Cordonnier C, Hirsch HH. 2017. ECIL guidelines for the prevention, diagnosis and treatment of BK polyomavirus-associated haemorrhagic cystitis in haematopoietic stem cell transplant recipients. J Antimicrob Chemother 73:12–21. https://doi.org/10.1093/jac/dkx324.
23. Hirsch HH, Kardas P, Kranz D, Leboeuf C. 2013. The human JC polyomavirus (JCPyV): virological background and clinical implications. APMIS 121:685–727. https://doi.org/10.1111/apm.12128.
24. Ho J, Jedrych JJ, Feng H, Natalie AA, Grandinetti L, Mirvish E, Crespo MM, Yadav D, Fasanella KE, Proksell S, Kuan SF, Pastrana DV, Buck CB, Shuda Y, Moore PS, Chang Y. 2015. Human polyomavirus 7-associated pruritic rash and viremia in transplant recipients. J Infect Dis 211:1560–1565. https://doi.org/10.1093/infdis/jiu524.
25. Hirsch HH, Babel N, Comoli P, Friman V, Ginevri F, Jardine A, Lautenschlager I, Legendre C, Midtvedt K, Munoz P, Randhawa P, Rinaldo CH, Wieszek A, ESCMID Study Group of Infection in Compromised Hosts. 2014. European perspective on human polyomavirus infection, replication and disease in solid organ transplantation. Clin Microbiol Infect 20(Suppl 7):S74–S88. https://doi.org/10.1111/1469-0691.12538.
26. White MK, Gordon J, Khalili K. 2013. The rapidly expanding family of human polyomaviruses: recent developments in understanding their life cycle and role in human pathology. PLoS Pathog 9:e1003206. https://doi.org/10.1371/journal.ppat.1003206.
27. Siebrasse EA, Nguyen NL, Smith C, Simmonds P, Wang D. 2014. Immunohistochemical detection of KI polyomavirus in lung and spleen. Virology 468-470:178–184. https://doi.org/10.1016/j.virol.2014.08.005.
28. Siebrasse EA, Nguyen NL, Willby MJ, Erdman DD, Menegus MA, Wang D. 2016. Multiorgan WU polyomavirus infection in bone marrow transplant recipient. Emerg Infect Dis 22:24–31. https://doi.org/10.3201/eid2201.151384.
29. Siebrasse EA, Pastrana DV, Nguyen NL, Wang A, Roth MJ, Holland SM, Freeman AF, McDyer J, Buck CB, Wang D. 2015. WU polyomavirus in respiratory epithelial cells from lung transplant patient with Job syndrome. Emerg Infect Dis 21:103–106. https://doi.org/10.3201/eid2101.140855.
30. Schrama D, Groesser L, Ugurel S, Hafner C, Pastrana DV, Buck CB, Cerroni L, Theiler A, Becker JC. 2014. Presence of human polyomavirus 6 in mutation-specific BRAF inhibitor-induced epithelial proliferations. JAMA Dermatol 150:1180–1186. https://doi.org/10.1001/jamadermatol.2014.1116.
31. Nguyen KD, Lee EE, Yue Y, Stork J, Pock L, North JP, Vandergriff T, Cockerell C, Hosler GA, Pastrana DV, Buck CB, Wang RC. 2017. Human polyomavirus 6 and 7 are associated with pruritic and dyskeratotic dermatoses. J Am Acad Dermatol 76:932–940 e3. https://doi.org/10.1016/j.jaad.2016.11.035.
32. DeCaprio JA, Garcea RL. 2013. A cornucopia of human polyomaviruses. Nat Rev Microbiol 11:264–276. https://doi.org/10.1038/nrmicro2992.
33. Imperiale MJ, Jiang M. 2016. Polyomavirus persistence. Annu Rev Virol 3:517–532. https://doi.org/10.1146/annurev-virology-110615-042226.
34. Gosert R, Rinaldo CH, Funk GA, Egli A, Ramos E, Drachenberg CB, Hirsch HH. 2008. Polyomavirus BK with rearranged noncoding control region emerge in vivo in renal transplant patients and increase viral replication and cytopathology. J Exp Med 205:841–852. https://doi.org/10.1084/jem.20072097.
35. Ferenczy MW, Marshall LJ, Nelson CD, Atwood WJ, Nath A, Khalili K, Major EO. 2012. Molecular biology, epidemiology, and pathogenesis of progressive multifocal leukoencephalopathy, the JC virus-induced demyelinating disease of the human brain. Clin Microbiol Rev 25:471–506. https://doi.org/10.1128/CMR.05031-11.
36. Olsen GH, Hirsch HH, Rinaldo CH. 2009. Functional analysis of polyomavirus BK non-coding control region quasispecies from kidney transplant recipients. J Med Virol 81:1959–1967. https://doi.org/10.1002/jmv.21605.
37. Gosert R, Kardas P, Major EO, Hirsch HH. 2010. Rearranged JC virus non-

coding control regions found in progressive multifocal leukoencephalopathy patient samples increase virus early gene expression and replication rate. J Virol 84:10448–10456. https://doi.org/10.1128/JVI.00614-10.
38. Khan ZM, Liu Y, Neu U, Gilbert M, Ehlers B, Feizi T, Stehle T. 2014. Crystallographic and glycan microarray analysis of human polyomavirus 9 VP1 identifies N-glycolyl neuraminic acid as a receptor candidate. J Virol 88:6100–6111. https://doi.org/10.1128/JVI.03455-13.
39. Stroh LJ, Neu U, Blaum BS, Buch MH, Garcea RL, Stehle T. 2014. Structure analysis of the major capsid proteins of human polyomaviruses 6 and 7 reveals an obstructed sialic acid binding site. J Virol 88:10831–10839. https://doi.org/10.1128/JVI.01084-14.
40. Buck CB, Van Doorslaer K, Peretti A, Geoghegan EM, Tisza MJ, An P, Katz JP, Pipas JM, McBride AA, Camus AC, McDermott AJ, Dill JA, Delwart E, Ng TF, Farkas K, Austin C, Kraberger S, Davison W, Pastrana DV, Varsani A. 2016. The ancient evolutionary history of polyomaviruses. PLoS Pathog 12:e1005574. https://doi.org/10.1371/journal.ppat.1005574.
41. Bollag B, Chuke WF, Frisque RJ. 1989. Hybrid genomes of the polyomaviruses JC virus, BK virus, and simian virus 40: identification of sequences important for efficient transformation. J Virol 63:863–872.
42. Chen BJ, Atwood WJ. 2002. Construction of a novel JCV/SV40 hybrid virus (JCSV) reveals a role for the JCV capsid in viral tropism. Virology 300:282–290. https://doi.org/10.1006/viro.2002.1522.
43. Major EO, Miller AE, Mourrain P, Traub RG, de Widt E, Sever J. 1985. Establishment of a line of human fetal glial cells that supports JC virus multiplication. Proc Natl Acad Sci U S A 82:1257–1261. https://doi.org/10.1073/pnas.82.4.1257.
44. Tang WJ, Folk WR. 1989. Constitutive expression of simian virus 40 large T antigen in monkey cells activates their capacity to support polyomavirus replication. J Virol 63:5478–5482.
45. Henriksen S, Tylden GD, Dumoulin A, Sharma BN, Hirsch HH, Rinaldo CH. 2014. The human fetal glial cell line SVG p12 contains infectious BK polyomavirus. J Virol 88:7556–7568. https://doi.org/10.1128/JVI.00696-14.
46. Grundhoff A, Fischer N. 2015. Merkel cell polyomavirus, a highly prevalent virus with tumorigenic potential. Curr Opin Virol 14:129–137. https://doi.org/10.1016/j.coviro.2015.08.010.
47. Bethge T, Hachemi HA, Manzetti J, Gosert R, Schaffner W, Hirsch HH. 2015. Sp1 sites in the noncoding control region of BK polyomavirus are key regulators of bidirectional viral early and late gene expression. J Virol 89:3396–3411. https://doi.org/10.1128/JVI.03625-14.
48. Zhao L, Imperiale MJ. 2017. Identification of Rab18 as an essential host factor for BK polyomavirus infection using a whole-genome RNA interference screen. mSphere 2(4):e00291-17. https://doi.org/10.1128/mSphereDirect.00291-17.
49. Bethge T, Ajuh E, Hirsch HH. 2016. Imperfect symmetry of Sp1 and core promoter sequences regulates early and late virus gene expression of the bidirectional BK polyomavirus noncoding control region. J Virol 90:10083–10101. https://doi.org/10.1128/JVI.01008-16.
50. Cartharius K, Frech K, Grote K, Klocke B, Haltmeier M, Klingenhoff A, Frisch M, Bayerlein M, Werner T. 2005. MatInspector and beyond: promoter analysis based on transcription factor binding sites. Bioinformatics 21:2933–2942. https://doi.org/10.1093/bioinformatics/bti473.
51. Ehlers B, Moens U. 2014. Genome analysis of non-human primate polyomaviruses. Infect Genet Evol 26:283–294. https://doi.org/10.1016/j.meegid.2014.05.030.
52. Neumann F, Borchert S, Schmidt C, Reimer R, Hohenberg H, Fischer N, Grundhoff A. 2011. Replication, gene expression and particle production by a consensus Merkel cell polyomavirus (MCPyV) genome. PLoS One 6:e29112. https://doi.org/10.1371/journal.pone.0029112.
53. Martel-Jantin C, Filippone C, Cassar O, Peter M, Tomasic G, Vielh P, Briere J, Petrella T, Aubriot-Lorton MH, Mortier L, Jouvion G, Sastre-Garau X, Robert C, Gessain A. 2012. Genetic variability and integration of Merkel cell polyomavirus in Merkel cell carcinoma. Virology 426:134–142. https://doi.org/10.1016/j.virol.2012.01.018.
54. Lednicky JA, Butel JS, Luetke MC, Loeb JC. 2014. Complete genomic sequence of a new human polyomavirus 9 strain with an altered noncoding control region. Virus Genes 49:490–492. https://doi.org/10.1007/s11262-014-1119-z.
55. Pipas JM. 1992. Common and unique features of T antigens encoded by the polyomavirus group. J Virol 66:3979–3985.
56. Lynch KJ, Frisque RJ. 1990. Identification of critical elements within the JC virus DNA replication origin. J Virol 64:5812–5822.
57. Moens U, Van Ghelue M, Ludvigsen M, Korup-Schulz S, Ehlers B. 2015. Early and late promoters of BK polyomavirus, Merkel cell polyomavirus, trichodysplasia spinulosa-associated polyomavirus and human polyomavirus 12 are among the strongest of all known human polyomaviruses in 10 different cell lines. J Gen Virol 96:2293–2303. https://doi.org/10.1099/vir.0.000181.
58. Schmidt K, Keiser S, Gunther V, Georgiev O, Hirsch HH, Schaffner W, Bethge T. 2016. Transcription enhancers as major determinants of SV40 polyomavirus growth efficiency and host cell tropism. J Gen Virol 97:1597–1603. https://doi.org/10.1099/jgv.0.000487.
59. Keiser S, Schmidt K, Bethge T, Steiger J, Hirsch HH, Schaffner W, Georgiev O. 2015. Emergence of infectious simian virus 40 whose AT tract in the replication origin/early promoter region is substituted by cellular or viral DNAs. J Gen Virol 96:601–606. https://doi.org/10.1099/vir.0.071274-0.
60. Rinaldo CH, Hirsch HH. 2013. The human polyomaviruses: from orphans and mutants to patchwork family. APMIS 121:681–684. https://doi.org/10.1111/apm.12125.
61. Ehlers B, Wieland U. 2013. The novel human polyomaviruses HPyV6, 7, 9 and beyond. APMIS 121:783–795. https://doi.org/10.1111/apm.12104.
62. Moens U, Seternes OM, Hey AW, Silsand Y, Traavik T, Johansen B, Rekvig OP. 1995. In vivo expression of a single viral DNA-binding protein generates systemic lupus erythematosus-related autoimmunity to double-stranded DNA and histones. Proc Natl Acad Sci U S A 92:12393–12397. https://doi.org/10.1073/pnas.92.26.12393.
63. Harborth J, Elbashir SM, Bechert K, Tuschl T, Weber K. 2001. Identification of essential genes in cultured mammalian cells using small interfering RNAs. J Cell Sci 114:4557–4565.